A cysteine-rich domain of the Cuf1 transcription factor is required for high copper stress sensing and fungal virulence

Corinna Probst [1], Catherine A. Denning-Jannace[4], Lukas M. du Plooy[2], Charles Giamberardino[1], Yohannes Asfaw[5] Katherine J. Franz[4], J. Andrew Alspaugh [1,2,3*]

Duke University School of Medicine, Durham, NC, USA: Departments of Medicine[1], Molecular Genetics and Microbiology[2], and Cell Biology[3]

Duke University, Durham, NC, USA: Department of Chemistry[4]

Duke University, Durham, NC: Division of Laboratory Animal Resources[5]

Running title: **High copper sensing in the human fungal pathogen *Cryptococcus neoformans***

Keywords: **cell wall, nutritional immunity, metal homeostasis, fungal pathogenesis**

(*) Corresponding Author: J. Andrew Alspaugh, andrew.alspaugh@duke.edu

Abstract

The ability to sense, import but also detoxify copper (Cu) has been shown to be crucial for microbial pathogens to survive within the host. Previous studies conducted with the opportunistic human fungal pathogen *Cryptococcus neoformans* (*Cn*) have revealed two extreme Cu environments encountered during infection: A high Cu environment within the lung and a low Cu environment within the brain. However, how *Cn* senses these different host Cu microenvironments, and the consequences of a blunted Cu stress adaption for pathogenesis, are not well understood.

In contrast to other fungi, *Cn* has a single transcription factor, Cuf1, to regulate adaptive responses to both high- and low-Cu stress. Sequence analysis of *Cn* Cuf1 identified three conserved cysteine (Cys)-rich regions that may play a role in Cu sensing. We mutated the 1st Cys-rich region within the *CUF1* gene to investigate its role for *Cn* high Cu stress sensing. Subsequent analysis of Cuf1 transcriptional activity and target gene promoter binding demonstrated that the 1st Cys-rich region is required for Cuf1 transcriptional activity in high Cu stress. We performed an inhalational murine infection to analyze the effects of a blunted high Cu stress response on pathogenesis. No significant differences in lung fungal burden were observed based on variable Cuf1 activity. However, strains with defective high Cu stress regulation induced a markedly altered immune response in mice. Based on these findings, we hypothesize that Cuf1-driven high Cu responses are not required for initial survival but instead modulate immune recognition and inflammation within the mouse lung.

35 **Importance**

36 Copper is an essential micronutrient required for survival in all kingdoms of life as it is used as a
37 catalytic cofactor for many essential processes in the cell. In turn, this reactivity of copper ions makes
38 elevated levels of free copper toxic for the cell. This dual nature of copper-essential for life but toxic at
39 elevated levels- is used by our innate immune system in a process called nutritional immunity to combat
40 and kill invading pathogens. In this work we explore how the fungal human pathogen *Cryptococcus*
41 *neoformans* senses high copper stress, a copper microenvironment encountered within the host lung.
42 We identified a specific cysteine-rich region within the copper responsive transcription factor Cuf1 to be
43 essential for high copper stress sensing. Mutation of this region led to an impaired high copper stress
44 adaptation, which did not affect fitness of the yeast but did impact immune recognition and
45 inflammation inside the host lung.

46

47 **Introduction**

48 Copper (Cu) is an essential trace element in both microbes and mammalian cells, serving as a
49 catalytic cofactor for a diverse range of cellular processes including iron uptake and distribution;
50 mitochondrial cytochrome oxidase activity; Cu, Zinc (Zn) superoxide dismutase catalysis; and melanin
51 pigment production [1, 2]. Although Cu is required for life, elevated Cu levels are toxic due to its ability
52 to induce uncontrolled redox cycling, causing the formation of toxic reactive oxygen species (ROS) and
53 oxidative damage of DNA, proteins, and lipids [3, 4]. Free Cu ions were also shown to induce protein
54 aggregation, triggering protein miss-folding and precipitation [5, 6]. Furthermore, Cu has been shown to
55 irreversibly displace iron (Fe) from Fe-S-cluster containing proteins, rendering these proteins non
56 functional [7, 8]. Therefore, organisms have evolved processes to sense and tightly regulate cellular Cu
57 availability, to maintain but not exceed the required cellular Cu quota [2, 4, 9-11].

58 Pathogenic microbes encounter unique extremes of Cu stress. Infected hosts often employ Cu-
59 sequestering strategies known as "nutritional immunity" to limit Cu availability for invading pathogens
60 [12-17]. In other sites, such as the macrophage phagolysosome, the host ATP7A Cu pump actively
61 imports Cu to toxic concentrations to kill engulfed microorganisms [18] and, more recently, Mohamed
62 and colleagues demonstrated that brain resident microglia provide Cu to a phagocytosed fungal
63 pathogen in the central nervous system (CNS) [13].

64 The basidiomycete *Cryptococcus neoformans* (*Cn*) is an opportunistic fungal pathogen that causes
65 life-threatening disease in immune compromised individuals [19, 20]. *Cn* is an environmental fungus
66 frequently isolated from degrading plants, and soil contaminated with bird guano. Infectious spores or
67 desiccated yeast cells are inhaled by mammalian hosts from the environment, resulting in an initial
68 pulmonary infection [20]. In patients with weakened immune systems, including those with late-stage
69 HIV infection, *Cn* disseminates through the bloodstream, crosses the blood-brain barrier, and colonizes
70 the brain, where it causes lethal infection [19, 20]. Previous studies have revealed that *Cn* encounters
71 two extreme Cu environments during infection. During the initial infection within the lung, *Cn* senses a
72 high Cu environment. In contrast, once the microorganism reaches the CNS, it senses low Cu availability
73 [21, 22]. Thus, to maintain its proper cellular Cu quota, *Cn* needs to switch from Cu-detoxification during
74 pulmonary infection to Cu-acquisition upon entering the CNS.

75 Several adaptive strategies for *Cn* Cu homeostasis have been described. To combat high Cu stress, *Cn*
76 induces the Cu-detoxifying metallothionein genes *MT1* and *MT2*, the ROS detoxifying superoxide
77 dismutase (*SOD*) 1 gene, as well as *ATM1,* a gene encoding a mitochondrial ABC transporter required to
78 provide a sulfuric precursor for cytosolic Fe-S cluster biosynthesis [23]. These genes were previously
79 shown to be required for *Cn* survival inside macrophages or in a mouse model of *cryptococcosis* [21, 24-
80 26]. To combat the Cu-restrictive CNS environment, *Cn* induces its two high affinity copper importer
81 genes *CTR1* and *CTR4*, as well as the *CBI1* gene, encoding a Cu-binding protein required for efficient Cu

82 acquisition [22, 27, 28]. Additionally, Smith and colleagues described a transcription factor-mediated
83 switch between the Cu/Zn-dependent Sod1 and a Cu-independent/ manganese (Mn)-dependent Sod2 to
84 prioritize Cu towards other required Cu-dependent pathways when labile Cu is limited [11]. Even though
85 these adaptive strategies have been described, it is still unclear how they function together to facilitate
86 adaption against the encountered host Cu microenvironment and how failure of adaption to high or low
87 Cu stress effects *Cn* survival and pathogenesis.

88 Interestingly, most fungi employ two distinct transcription factors to control responses to high and
89 low Cu stress [2]. For example, the *Saccharomyces cerevisiae* (*Sc*) Ace1 transcription factor is activated in
90 a high Cu environment to regulate gene expression to protect the yeast from toxic Cu levels [29, 30],
91 while the *Sc* Mac1 transcription factor is activated by low Cu environments to favor Cu acquisition [31].
92 In contrast, *Cn* maintains a single Cu-responsive transcription factor Cuf1, that controls both high and
93 low Cu stress responsive genes [23]. Deletion of *CUF1* renders *Cn* less virulent in an intravenous mouse
94 model of *cryptococcosis* [32], further underscoring the importance of Cu homeostasis in *Cn* pathogenesis
95 and suggests the potential of Cuf1 as a fungal-specific intervention target to disrupt pathogen-driven
96 adaptions in the host nutritional environment during infection. However, the actual mechanism of gene
97 regulation by Cuf1 in response to various Cu stresses is not well understood and has yet to be
98 elucidated.

99 Sequence comparison between *Cn*Cuf1 and other fungal Cu-responsive transcription factors
100 identified the highest homology within the first 39 amino acids (aa) of the N-terminal domain [23]. This
101 region includes a Zn-binding motif and the highly conserved positively charged 'KGRP' motif that is
102 crucial for binding the minor groove of the DNA binding sites [29, 31, 33-36]. Mutational studies in
103 *Cn*Cuf1 have demonstrated that the KGRP motif is required for regulation of both high and low Cu
104 responses, consistent with the role of Cuf1 in transcription under both conditions [23]. Following the
105 minor groove binding region, the similarity between Cuf1 and other Cu-responsive transcription factors

106 decreases considerably, except for three cysteine (Cys)-rich regions: The first Cys-rich region is similar to
107 the Cys-rich region found in the high Cu-responsive transcription factor *Sc*Ace1. The second and third
108 Cys-rich regions are not found in *Sc*Ace1 but are conserved in the low Cu-responsive transcription factor
109 *Sc*Mac1 [23]. A role in Cu-binding and regulation of transcriptional activity has been established for the
110 Cys-rich regions in *Sc*Ace1 and *Sc*Mac1. In both cases Cu binding to the Cys-rich region of these
111 transcription factors acts as an ON-OFF switch either activating (Ace1-like transcription factors) or
112 deactivating (Mac1-like transcription factors) transcriptional activity [29, 33, 34, 37]. However, in
113 contrast to Ace1- and Mac1-like transcription factors, *Cn*Cuf1 binds and regulates genes in response to
114 low and high Cu stress, and additionally is bound constitutively to a rather unexpected subset of genes,
115 regardless of the encountered Cu stress [23]. These findings point towards a more complex regulation of
116 Cuf1 dependent gene regulation. Specifically, a single transcription factor must be activated by a specific
117 Cu stress condition to bind to and direct gene expression of its target genes, but also has to be activated
118 by the opposed Cu stress condition where it also has to bind to and direct gene expression of a
119 completely different set of target genes, while still being bound constitutively at a small subset of
120 promoters independent of the present Cu stress. Consequently, the requirements of Cuf1 transcriptional
121 activity at high and low Cu stress suggests a more multi-faceted model of gene regulation than the
122 ON/OFF model previously described for Ace1- or Mac1-like transcription factors.

123 Here we present an initial study of the role of the Ace1-like Cys site for high Cu stress sensing and
124 gene regulation by *Cn*Cuf1. We analyzed the consequential role of a blunted high Cu stress response for
125 cupro-enzyme regulation *in vitro* and its effects on pathogenesis *in vivo* within the mouse lung
126 environment using an inhalational mouse model of *cryptococcosis*.

127

128 **RESULTS**

129 **Mutation of the Ace1-like Cys site in the Cuf1 transcription factor renders the fungus susceptible to**
130 **high Cu stress.**

131 Cuf1 is the central Cu-responsive transcription factor known to regulate high and low copper genes in
132 *Cn*. Previous research conducted on other fungal transcription factors implicates conserved Cys-rich
133 motifs to bind Cu and regulate transcriptional activity in response to cellular Cu levels [29, 33, 34, 37]
134 (Fig1 A). The first Cys-rich region encoded by *CUF1* is formed by an 11 aa motif, containing 4 cysteines,
135 which are highly conserved among Cuf1 and Ace1-like transcription factors [23]. To elucidate how Cuf1
136 senses high Cu and is guided to its target genes in response to high Cu stress, we mutated all 4
137 conserved Cys located in the Ace1-like Cys rich region to alanine (Cuf1-FLAG ΔAce1, Fig 1A). Alleles
138 encoding FLAG-tagged versions of the Cuf1 wild type (WT) protein and the Cuf1 ΔAce1 mutant were
139 incorporated into the *cuf1Δ* mutant strain at the same genomic site (safe haven 1), both expressed by
140 the *CUF1* promoter (Fig 1A-B).

141 To explore the effects of the Ace1-like Cys site mutation on Cuf1-FLAG protein levels at high and low
142 Cu stress, we conditioned the *CUF1*-FLAG WT and two independent *CUF1-FLAG* ΔAce1 strains for 3h in
143 either SC medium + 1 mM $CuSO_4$ (= high Cu) or SC medium + 1 mM of the extracellular Cu chelator
144 bathocuproinedisulfonic acid (BCS,= low Cu) at 30°C. Western blot analysis using a FLAG-HRP conjugate
145 demonstrated no differences in Cuf1-FLAG protein levels in response of high or low Cu stress between
146 the WT or the Ace1- like Cys site mutant proteins, indicating that the Ace1-like site mutation does not
147 affect Cuf1 protein levels (Fig 1C).

148 To determine the physiological effects of the Ace1-like Cys-rich region on regulation of Cu
149 homeostasis during Cu stress, we assessed the ability of each allele to complement the *cuf1Δ* growth
150 phenotype in high and low Cu stress environments. In all stress conditions, the *CUF1-FLAG* WT allele
151 fully restored growth of the *cuf1Δ* mutant strain, demonstrating that the FLAG-tag did not compromise

152 Cuf1 protein function. Similarly, *CUF1-FLAG* ΔAce1 complemented the *cuf1Δ* growth defect in Cu-limiting
153 conditions, however it failed to restore growth in a high Cu environment (Fig1D). This finding suggests a
154 specific role for the Ace1- like Cys rich region for regulating transcriptional activity in response to high Cu
155 stress.

156

157 **The Ace1-like Cys site is required for Cuf1 to specifically bind to and regulate high Cu responsive genes**

158 To test whether the growth phenotype observed under high Cu for both the *cuf1*Δ strain and
159 the *cuf1*Δ strain expressing the *CUF1*-FLAG ΔAce1 allele were due to a similar failure to activate Cuf1
160 target genes in response to high Cu stress, we assessed transcript levels for established high and low Cu
161 regulated genes in each strain. The *MT1* gene encoding the Cu detoxifying metallothionein 1 protein and
162 the *ATM1* gene, encoding for a mitochondrial inner membrane ABC transporter involved in cytosolic Fe-
163 S assembly, were used to assess transcriptional responses to high Cu stress [21, 24]; and the *CTR4* gene,
164 encoding a high affinity Cu importer, and the *CBI1* gene, encoding the copper binding and release
165 protein 1, were used to assess responses to low Cu stress [22, 23, 27]. The WT and the *cuf1Δ* mutant
166 strain, as well as the *cuf1Δ* mutant strain expressing either *CUF1-FLAG* WT or the *CUF1-FLAG*-ΔAce1
167 mutant allele, were incubated for 3h in SC medium supplemented with either 1 mM $CuSO_4$ (=high Cu) or
168 1 mM BCS (=low Cu) at 30°C prior to RNA extraction. Transcript levels of the Cu-response genes for each
169 strain in each condition were determined by quantitative real-time PCR (qRT-PCR). Consistent with prior
170 results, the *MT1* and *ATM1* genes were induced in the WT strain under high Cu conditions, and the *CTR4*
171 and *CBI1* genes were induced in low Cu conditions (Fig 2 A-B) [23]. In contrast, the transcript levels of
172 both high Cu and low Cu genes were not induced in either condition in the *cuf1*Δ mutant. The *CUF1-*
173 *FLAG* WT strain fully restored gene expression in both conditions. However, consistent with the
174 observed growth phenotype on high Cu media, mutation of the Ace1-like Cys site was associated with

175 defective transcriptional activation of high Cu-regulated genes (*MT1* and *ATM1*, Fig 2 A), while fully
176 restoring WT transcript levels of genes involved in low Cu stress response (*CTR4* and *CBI1,* Fig 2 B).

177 The Cuf1 transcription factor was previously demonstrated to directly bind the promoters of
178 these high and low Cu reporter genes [23]. We used chromatin immunoprecipitation followed by qRT-
179 PCR analysis (ChIP-PCR) to determine whether the observed differential transcript levels in each strain
180 were associated with changes in Cuf1 promoter binding. We specifically chose oligonucleotides
181 corresponding to the *CTR4* and *MT1* promoters as indicators of low- and high-Cu stress gene promoter
182 binding, respectively. To do so, we incubated the strains in the identical high- and low-Cu stress
183 conditions as above prior to protein-DNA crosslinking and chromatin immunoprecipitation. Enrichment
184 of the *MT1* or *CTR4* promoter fragments in each sample was calculated relative to the WT strain and was
185 further normalized against the *TUB1* tubulin gene as a non Cuf1 target gene. Consistent with previous
186 studies, we observed a significant enrichment of the *MT1* promoter, but not the *CTR4* promoter, in the
187 Cuf1-FLAG WT sample conditioned in high Cu stress and enrichment of the *CTR4* promoter sequence
188 during low Cu stress [23](Fig 2C-D). In contrast, no enrichment of the *MT1* promoter was observed by
189 ChIP-PCR in the *cuf1*Δ + *CUF1-FLAG* ΔAce1 strain conditioned in high Cu stress, whereas the *CTR4*
190 promoter was enriched in this strain to similar levels as in the Cuf1-FLAG WT allele expressing strain (Fig
191 2C-D). Taken together, these data show that the Ace1-like Cys-rich region is required for Cuf1 binding to
192 and regulation of high Cu-responsive promoters while it does not impact binding or regulation of low
193 Cu-responsive promoters.

194 Unlike other Cu-responsive transcription factors, Cuf1 does not only bind and regulate specific
195 gene promoters at either low and high Cu conditions. It also constitutively binds the promoters of a
196 group of genes regardless of changes in Cu concentration [23]. We therefore performed transcript and
197 Cuf1-promoter binding analysis for a subset of these genes (*CDA2*, *CFO1*) in both Cu stress conditions
198 (Supp. Fig 1). The Chitin deacetylase 2 (Cda2) was previously described to be involved in chitosan

199 synthesis within the lung environment [38]. *CDA2* was identified as a Cuf1-regulated gene, with Cuf1
200 binding of its promoter at high and low Cu levels and a modest but statistically significant transcript
201 induction only during high Cu stress [23]. The ferroxidase gene (*CFO1*), which is involved in high affinity
202 iron uptake [39], was likewise identified to have constitutive promoter binding by Cuf1. However, in
203 contrast to *CDA2*, *CFO1* is induced by low Cu stress [23]. In line with previous published RNAseq data, we
204 observed a decrease in *CDA2* transcript in the *cuf1*Δ mutant strain in presence of high Cu stress which
205 was restored by the expression of the WT *CUF1-FLAG* allele, but not the *CUF1-FLAG*-ΔAce1 mutant allele
206 (Supp Fig 1A), indicating a role for the Ace1-like site in Cuf1-dependent regulation of the *CDA2* gene
207 during high Cu stress. However, in contrast to *MT1* or *CTR4,* no Cuf1-associated enrichment of the *CDA2*
208 promoter fragment was found by ChIP-PCR at either stress condition (Supp. Fig 2B-C).

209 In contrast to *CDA2*, which seemed to be only regulated by Cuf1 during high Cu stress, we
210 observed a ~55% reduction of the *CFO1* transcript level in the *cuf1*Δ background in both Cu stress
211 conditions, suggesting *CFO1* expression to be constitutively driven by Cuf1 (Supp. Fig 1A). *CFO1*
212 transcript levels were mostly restored in the *cuf1*Δ mutant by the expression of either the WT *CUF1-*
213 *FLAG* allele or the *CUF1-FLAG* ΔAce1 mutant allele (Supp Fig 1A). Similar to *CDA2* promoter binding, no
214 enrichment of the *CFO1* promoter fragment was found in cells conditioned with high Cu stress
215 conditions in either strains (Supp. Fig 2B). However, we did observe a modest enrichment of the *CFO1*
216 promoter at low Cu stress, independent from the absence or presence of the Ace1-like Cys site (Supp.
217 Fig1C). This finding suggests that, in contrast to Cuf1-target genes whose promoters are bound
218 exclusively by Cuf1 during high Cu stress, the Ace1-like Cys site is not absolutely required to support
219 *CFO1* expression in the presence of high Cu stress.

220 Together, these transcript and promoter binding data demonstrate that the Ace1-like Cys site is
221 required for the Cuf1 transcription factor to transcriptionally activate high Cu-responsive genes but not

222 low Cu-responsive genes. This activity likely explains the defective cellular adaptation to high Cu stress
223 for strains with mutations of this site.

224

225 **The Ace1-like Cys site is required for proper regulation of ROS detoxification and melanization in high**
226 **Cu environments.**

227 *Cn* encounters both low- and high-Cu microenvironments in the infected host [22]. We therefore
228 assessed the role of Cuf1 and the Ace1-like Cys region in the activity of cupro-enzymes required for *Cn*
229 stress resistance and survival within these microenvironments in the human host.

230 Laccase 1 and melanin production:

231 The *Cn* Lac1 protein is a Cu-containing diphenol oxidase/laccase involved in formation of
232 melanin, a cell wall-associated pigment that protects the fungal from host-derived oxidative and
233 nitrosative stress as well as from antifungal drugs [40]. The process of melanization is tightly linked to Cu
234 homeostasis and Cuf1 in multiple ways. First, melanin production requires cellular Cu as Lac1 oxidase
235 activity is dependent on Cu as a catalytic cofactor [41]. Second, *LAC1* gene expression is controlled in a
236 Cuf1-dependent manner [23, 28, 42, 43](Fig 3A). To analyze the effects of the Ace1-like Cys site
237 mutation on melanin production, we performed a combination of an *in vitro* pigmentation assay using L-
238 DOPA media plates supplemented with BCS or $CuSO_4$ to create a Cu limiting or Cu excess environment as
239 well as *LAC1* transcript analysis in L-DOPA medium in the presence of Cu limitation or excess (Fig 3B-D).

240 To test for melanin production, we incubated the WT strain, the *cuf1*Δ mutant, and the *cuf1*Δ
241 strain expressing either *CUF1-FLAG* WT or the ΔAce1-like Cys site mutant allele on L-DOPA medium
242 supplemented with either 10 µM BCS (to slightly restrict Cu) or 10 µM $CuSO_4$ (to provide excess Cu). As
243 controls, we included the completely melanin-defective *lac1*Δ mutant strain and the *cbi1*Δ *ctr4*Δ double

244 mutant strain that is impaired in copper import [27, 41]. For each strain, relative *LAC1* transcript levels
245 were measured after 3h of incubation in liquid L-DOPA medium similarly supplemented with either 10
246 µM BCS or 10 µM $CuSO_4$.

247 The WT strain was strongly melanized by 72h, and the addition of excess Cu to the medium
248 resulted in a higher degree of pigmentation (Fig 3B). In contrast, the *cuf1*Δ mutant displayed decreased
249 melanin in Cu-limited conditions, similar to that of the *cbi1*Δ *ctr4*Δ Cu import mutant (Fig 3B). In these
250 conditions, *LAC1* gene expression in the *cuf*1Δ mutant is similar to WT, suggesting that its decreased
251 melanin formation is due to failed induction of Cu import genes, such as *CTR4*, resulting in reduced
252 levels of intracellular Cu (Fig 3 C-D). Consistent with this hypothesis, we observed full restoration of
253 melanization in the Cu-import mutant, when Cu is supplemented to the L-DOPA medium, restoring Lac1
254 Cu loading and thus function (Fig 3B).

255 In contrast to the Cu import mutant, melanin formation was not restored in the *cuf1*Δ mutant
256 when the medium was supplemented with Cu. On the contrary, the *cuf1*Δ strain demonstrated an even
257 more severe melanin-deficient phenotype, similar to that of the *lac1*Δ mutant (Fig 3 B). In this condition,
258 we observed a marked relative decrease in *LAC1* transcript levels in the *cuf1*Δ mutant strain, consistent
259 with the role of Cuf1 supporting *LAC1* expression when Cu is in excess. (Fig 3C).

260 Reintroduction of the *CUF1-FLAG* WT allele fully restored WT levels of melanin production in
261 both high and low Cu environments, as well as WT levels of *LAC1* and *CTR4* expression (Fig 3B-D). In
262 contrast, the *cuf1*Δ strain expressing the ΔAce1-like Cys site mutant allele only restored melanization
263 when Cu was limited but not when Cu was in excess (Fig 3B). In this strain, *CTR4* expression was fully
264 restored in Cu-limiting conditions, but *LAC1* expression was not restored in Cu excess (Fig 3C-D). Taken
265 together, these data demonstrate a major role for Cuf1 in controlling melanin formation, by ensuring
266 adequate levels of Cu as catalytical cofactor for Lac1 in low Cu conditions, and by supporting *LAC1* gene

267 expression in high Cu conditions. Additionally, the Cuf1 Ace1-like Cys site is required for ensuring proper
268 *LAC1* expression and melanization when Cu is in excess but is not required for melanization during Cu
269 limitation.

270 Superoxide dismutase and ROS detoxification:

271 The Cu,Zn-superoxide dismutase Sod1 helps to protect the fungal cell from ROS generated by
272 host immune cells during infection [26]. Previous studies demonstrated that Cuf1 binds to the *SOD1*
273 promoter in high Cu stress and induces *SOD1* gene expression. In contrast, during prolonged Cu
274 starvation, *SOD1* expression is repressed to divert limited Cu to other cell processes. In this condition,
275 Cuf1 binds to the *SOD2* promoter and induces the expression of a cytosolic retained variant of the Mn-
276 dependent mitochondrial superoxide dismutase 2 (Sod2) to uncouple ROS detoxification from a Cu-
277 requiring enzyme when cellular Cu is scarce [11]. Therefore, deletion of *CUF1* renders the cells
278 vulnerable to ROS stress not only during high Cu stress due to failure of up-regulation of *SOD1* but also
279 during low Cu stress due to inability to switch to a Cu-independent ROS detoxification pathway (Fig 4A).

280 To test effects of the Ace1-like Cys site mutation on cellular ROS detoxification, we incubated
281 the WT and *cuf1*Δ strains as well as strains expressing *CUF1-FLAG* WT or the ΔAce1-like Cys mutant allele
282 in the presence of increasing concentrations of the superoxide-generating compound menadione by disk
283 diffusion (Fig 4B). Consistent with previous studies, the *cuf1*Δ mutant showed an increased susceptibility
284 to menadione, measured by zone size of growth inhibition, in high or low Cu conditions (Fig 4C) [11].
285 Both Cu-stress phenotypes were fully restored in the *cuf1*Δ strain expressing the *CUF1-FLAG* WT allele.
286 In contrast, the strain expressing the *CUF1-FLAG* ΔAce1-like Cys site mutant allele only restored the ROS
287 resistance during low Cu stress but not high Cu stress (Fig 4C).

288 To fully analyze the role of the Ace1-like Cys site in regulating Sod-driven ROS detoxification, we
289 measured Sod activity in whole cell extracts using an in-gel Sod activity assay [10] from cells conditioned

290 in either low or high Cu stress. The Sod activity gels demonstrated three activity bands from cell extracts
291 from the WT strain incubated in low Cu conditions. The lowest band likely represents Sod1, while the
292 middle band likely represents Sod2 activity given their absence in the respective *sod1*Δ and *sod2*Δ
293 mutants (Fig 4D). The highest of the three bands was absent in the *cuf1*Δ and *sod2*Δ mutant strains (Fig
294 4D, yellow hash tag), and likely represents the cytosolic Sod2 variant that is specifically enriched in Cu
295 limitation in a Cuf1-dependent manner [11]. This Sod activity is restored in the *cuf1*Δ mutant by
296 introduction of either the *CUF1-FLAG* WT or the ΔAce1-like Cys site mutant allele, indicating that Cuf1-
297 dependent formation of cytosolic Sod2 during Cu-limiting conditions is not dependent on the Cuf1 Ace1-
298 like Cys site (Fig 4C-D).

299 The patterns of SOD activity varied when the strains were conditioned in high Cu stress, with
300 two predominant bands of similar intensity in WT cells. Both bands were significantly reduced in
301 intensity in the *cuf1*Δ mutant strain. Moreover, in the *sod1*Δ strain, these two bands were only faintly
302 present, and the upper of these two was either not present or altered in its molecular size (Fig 4D,
303 asterix), suggesting that this upper band represents Sod1 activity. While expression of *CUF1-FLAG* WT
304 restored the Sod activity bands to WT-like levels, we observed identical patterns of reduced Sod activity
305 in the *cuf1*Δ mutant as well as the *cuf1*Δ mutant expressing the *CUF1-FLAG* ΔAce1-Cys mutant allele,
306 indicating that the first Cys-rich site is required for Cuf1-depenedent induction of Sod1 protein activity in
307 response to high Cu stress (Fig 4D). Consistent with this finding, the Cuf1 Ace1-like Cys site is required
308 for supporting Cuf1-dependent *SOD1* transcript induction in high Cu conditions (Fig 4E). Together, these
309 phenotypic data, enzyme activity assays, and transcript assessments demonstrate the importance of the
310 Ace1-like Cys site for Cuf1-dependent regulation of ROS detoxification in a high Cu stress environment.

311

312 **Consequences of a blunted Cuf1 high Cu stress response on fitness and immune response inside the**
313 **host lung environment**

314 A previous study conducted by Waterman *et al.* established a role for Cuf1 for virulence in an
315 intravenous model of *Cn* infection, demonstrating a decreased fungal burden of the *cuf1*Δ mutant
316 compared to WT in the mouse brain but not in mouse lung [32]. More recent studies have suggested
317 that these different anatomic sites represent different Cu environments encountered by *Cn* during the
318 course of infection [21, 22, 27]. Using high and low Cu promoter driven Luciferase strains, one study
319 found an up-regulation of genes typically induced during Cu deficiency in the brain, while the lung
320 environment induced genes required for Cu detoxification [21]. This finding was further underscored by
321 assessing the effects of Cu homeostasis mutant strains on virulence and survival at the different sites of
322 infection: Strains lacking components of the Cu import machinery are less fit within the mouse brain
323 environment, while strains lacking components required for Cu detoxification are less fit in the mouse
324 lung environment [21, 22, 27].

325 Given the severe *in vitro* phenotypes found for the *cuf1Δ* mutant and the ΔAce1-like Cys site
326 mutant strain, we hypothesized that these strains would display altered physiology within the high Cu
327 environment of the lung. We inoculated female A/J mice by inhalation with the WT strain, the *cuf1*Δ
328 mutant, or the *cuf1*Δ mutant reconstituted with either the WT *CUF1-FLAG* allele or the *CUF1-FLAG*
329 ΔAce1 mutant allele. Lungs were harvested at 14 days of infection, a time at which lung infection is well
330 established but before animals succumb to the effects of a CNS infection, to assess lung fungal burden
331 as well as patterns of inflammation by histology (Fig 5). Consistent with prior studies, we did not observe
332 significant difference in lung fungal burden for any of the analyzed strains (Fig 5A) [32]. However, we did
333 note a significant increase in lung wet weight in animals infected with the WT or *CUF1-FLAG* WT strain
334 (Fig 5B). Additionally, we observed macroscopic differences between WT and *CUF1-FLAG* WT-infected

335 lungs compared to *cuf1*Δ- and the *CUF1-FLAG* ΔAce1-like Cys site mutant-infected lungs: WT-infected
336 lungs showed more frequent and larger foci of tissue abnormality compared to lungs infected with
337 either the *cuf1*Δ mutant or the ΔAce1-like Cys site mutant strain (Fig 5C, foci are indicated with white
338 arrows).

339 Histopathology analysis of fixed lung tissue confirmed altered immune reactions between these
340 two groups. Lungs infected with the WT strain displayed expected patterns of diffuse inflammation
341 surrounding single and grouped encapsulated yeast cells (Fig 5D) [44]. In the regions of most intense
342 inflammation, the inflammatory cell infiltration often obscured the clear definition of the underlying
343 alveolar structures. Titanized and non-titan yeast cells were observed throughout the lung tissue, both
344 in areas of inflammation as well as in surrounding less inflamed small airways and alveoli. In contrast
345 lungs infected with the *cuf1*Δ mutant strain displayed inflammation mostly confined to well
346 circumscribed foci, similar to the early granulomas described previously in studies of *Cn* strains with
347 slow growth phenotypes due to defects in mitochondrial function [44]. In these *cuf1*Δ-infected lungs, we
348 observed a sharp distinction between normal-appearing lung tissue and the foci of inflammation. Most
349 encapsulated yeast cells were present in these inflammatory foci with fewer fungal cells than WT
350 observed in the surrounding normal lung. Few titan cells were observed.

351 Lungs infected with *CUF1-FLAG* WT strain demonstrated very similar patterns of inflammation as
352 observed in WT-infected lungs. In contrast, the *CUF1-FLAG* ΔAce1-like Cys site mutant strain generated
353 an inflammatory response that had mixed features to both WT and *cuf1*Δ infections. Similar to *cuf1*Δ
354 infections, there was often a sharp distinction between inflamed and normal lung tissue with most yeast
355 cells observed in regions with the highest degree of inflammation. However, regions of inflammation
356 were less frequently circular, and there was more variability in yeast cell size than in the *cuf1*Δ
357 infections. Based on these findings, we hypothesize that Cuf1-regulated high Cu responses are not

358 required to colonize the mouse lung but modulate immune recognition and inflammation at the site of
359 infection.

360

361 ## Discussion

362 *Cn*Cuf1 is unique among fungal Cu-responsive transcription factors as it regulates a diverse
363 spectrum of Cu responses, combining the role of a high Cu-responsive transcription factor with the role
364 of a low Cu-responsive transcription factor [23]. Accordingly, it shares conserved motifs with both high
365 and low Cu-responsive transcription factors previously identified in ascomycete yeast Cu transcription
366 factors [23]. However, how these factors work together to regulate this rather complex Cuf1-driven Cu
367 response has not yet been elucidated. An interspecies cross-complementation study conducted with the
368 *Aspergillus fumigatus* (*Af*) AceA high Cu-responsive transcription factor demonstrated that AceA
369 homologs from ascomycete yeasts did not functionally complement the high Cu growth defect observed
370 in the *Af* Δ*aceA* mutant, suggesting that, even though the N-terminal DNA binding and the Cu sensing
371 motifs are highly conserved among these high Cu-responsive transcription factors, the motifs might
372 function differently in *Aspergillus* species than in their yeast counterparts [45]. This finding suggests that
373 despite using similar motifs/domains, different fungal clades may have evolved slightly different
374 molecular mechanisms to sense and/or transcriptionally regulate Cu stress responses. *Cn* Cuf1 is another
375 example of divergence of fungal Cu-responsive transcription factors, having evolved into a dual Cu-stress
376 responsive transcription factor by combining motifs from high- and low-Cu responsive transcription
377 factors with potentially yet unknown regulatory mechanisms.

378 The transition metal Cu has been established as an important virulence factor in all major
379 human fungal pathogens as it is used as a cofactor for several enzymes required for stress adaptation
380 within the host [10, 11, 40, 46, 47]. Consistently, Cu import genes and the Cu-responsive transcription

381 factors sensing and maintaining the cellular Cu quota were demonstrated to play a role in fungal
382 pathogenesis [22, 27, 32, 48-51]. For instance in *Candida albicans* (*Ca*), researchers demonstrated that
383 the low Cu-responsive *Ca*Mac1 transcription factor is required for host invasion, adhesion to host cells,
384 as well as antifungal tolerance [49]. Similarly, deletion of the low Cu-responsive MacA transcription
385 factor in *Af* attenuates pathogenicity in a neutropenic immunocompromised mice model [50].

386 Nutritional immunity responses for other transition metals mostly involve sequestering the
387 micronutrient from the site of infection [15, 17]. In contrast, Cu nutritional immunity responses appear
388 to be more dynamically regulated and are highly tissue dependent. While Cu might be restricted at one
389 site or time point of an infection, elevated and toxic Cu levels are present at other sites or time points to
390 act as an antimicrobial agent to kill the invading pathogen [10, 11, 13, 16, 21, 22, 48, 52]. Therefore, high
391 Cu stress responses are as important as Cu scavenging responses for pathogenesis. However, they must
392 be balanced to ensure proper adaptation to the Cu environment established at the particular infection
393 microniche.

394 Analysis of this dynamic shift of Cu nutritional immunity in the host and the fungal adaptive
395 stress response has been challenging to study in *Cn* since deletion of the *CUF1* gene ultimately blunts
396 both high and low Cu stress responses [23]. This makes deciphering the role of high and low Cu stress
397 responses during infection difficult as these stresses can have compensatory effects. For instance,
398 deletion of the *CTR4* Cu import gene was shown to be beneficial for *Cn* survival during pulmonary
399 infection, preventing an excessive influx of Cu and thus reducing the toxic effect of the high Cu lung
400 environment. In contrast, the same gene deletion resulted in reduced fungal virulence when the strain
401 was directly injected into the CNS, a site where Cu is limited [22]. Our mutational study aimed to identify
402 amino acid motifs specifically required for transcriptional activity in high Cu environments to uncoupled
403 Cuf1-driven high Cu stress responses from low Cu stress responses. In this work using a combination of
404 transcriptional analysis, Cu stress, and enzyme activity assays, we have established an essential role of

405 the Ace1-like Cys site for Cuf1 transcriptional activity during high Cu stress; mutation of this site does
406 not affect low Cu stress adaption. Using this site mutant, we were able to show the consequences of a
407 blunted high Cu stress adaptation on Cu-dependent virulence factors *in vitro* and on fungal growth and
408 immune recognition *in vivo.*

409 Recent work conducted with *Af*AceA demonstrated that mutation of its conserved Cys-rich
410 region attenuates virulence of the fungus similar to a Δ*aceA* mutant [45], highlighting the importance of
411 its Cys-rich region for activating Cu stress responses within the mouse lung environment. Similar to a
412 Δ*aceA* mutant in *Af*, deletion of the *CUF1* gene results in an attenuation of virulence [32]. However,
413 unlike the *Af* Δ*aceA* , a *CUF1* deletion did not affect *Cn* growth and survival inside the lung environment
414 [32, 45]. This observation stands in contrast with the severe *in vitro* phenotypes depicted by the *cuf1Δ*
415 mutant or the *CUF1-FLAG* ΔAce1 site mutant strains during high Cu stress. The observed *in vivo* growth
416 phenotype of the *cuf1Δ* and the *CUF1-FLAG* ΔAce1 mutant is also very different from the strongly
417 attenuated phenotype observed for a *Af* Δ*aceA* mutant. These very distinct outcomes of a blunted high
418 Cu stress response observed in the pathogenesis of two fungal pathogens in the same host environment
419 suggest different host-pathogen dynamics within the lung Cu environment, which are likely dependent
420 on the type of pathogen and its lifestyle inside the host tissue. Another possibility is that *Cn* might not
421 be as dependent on Cuf1 as *Af* on AceA for Cu detoxification *in vivo*. For instance, *Cn* could have evolved
422 alternate compensatory mechanisms to survive in the host lung environment which are independent
423 from Cuf1. To address these questions and to better understand the dynamics of Cu nutritional immune
424 responses within the lung environment, a more thorough assessment is needed at several different
425 stages of infection.

426 Although we did not observe significant differences in fungal burden between our WT and
427 mutant strains at two weeks of infection, we did observe macroscopic and microscopic differences
428 within the lungs of WT infected mice compared to mice infected with the *cuf1*Δ mutant or *CUF1-FLAG*

429 ΔAce1 site mutant. This observation suggests a role for Cuf1-driven high Cu stress responses for
430 modulating inflammatory responses within the lung environment, by mediating adaptive responses at
431 the fungal cell surface. This fungal feature is composed of ordered layers of polysaccharides and
432 mannosylated proteins and is the site of recognition and interaction with the host immune system:
433 Changes in carbohydrate composition as well as masking or unmasking of certain cell surface
434 components can modulate and define the pattern of inflammation caused by the pathogen [53-55]. For
435 instance, chitin has been associated with non-protective immune responses, and the degree of
436 unmasking coupled with the amount of chitosan within the *Cn* cell wall, modulates the severity of
437 immune recognition and inflammation within the host tissue [55, 56].

438 Previous work has suggested that the fungal cell wall plays a role in regulating intracellular Cu
439 levels during Cu stress [28]. In turn, Cuf1 regulates multiple genes associated with the fungal cell wall in
440 response to Cu stress [23, 28]. One example of these Cu-regulated cell wall genes is the chitin
441 deacetylase *CDA2,* an enzyme involved in chitosan synthesis. Our study suggests that *CDA2* is up-
442 regulated in response to high Cu stress and that this transcriptional activation is blunted in the *cuf1*Δ
443 null and ΔAce1-site mutant. Another study showed that cell wall architecture and cell wall chitosan
444 levels are significantly altered in a Cu homeostasis mutant strain during Cu limitation [28]. These findings
445 document a role for Cuf1 in modulating the fungal cell wall and in particular cell wall chitosan levels as
446 part of its Cu homeostasis response towards Cu stress. In this way, strains lacking chitosan in their cell
447 wall were shown to be more sensitive to high Cu stress [28]. We therefore propose a model in which
448 the observed differences in inflammatory patterns between WT-infected groups and the *cuf1*Δ mutant-
449 infected groups are caused by Cuf1-driven cell surface changes in response to the lung Cu environment.
450 We hypothesize that either loss of *CUF1* or simply a blunted high Cu-response prevents Cu-stress-driven
451 cell wall remodeling. This in turn, triggers a more focal, granuloma-like inflammatory response with
452 fungal containment within these inflammatory foci. Further investigations will more precisely define the

453 effects of Cu and Cuf1 on the fungal cell surface and their subsequent effects on fungal recognition and

454 inflammation at different stages and sites of infection.

455 # Material and Methods

456

457 **Ethics statement**

458 All animal experiments conducted in this study were approved by the Duke University
459 Institutional Animal Care and Use Committee (IACUC) (protocol #A102-20-05). Mice were handled
460 according to IACUC guidelines.

461

462 **Strains, media and growth conditions**

463 *Cryptococcus neoformans* strains used in this study are shown in **Table S1.** Strains generated in
464 this study were created using the *C. neoformans var. grubii H99* background. Strains were created using
465 biolistic transformation as previously described [57]. Yeast extract (2%)-peptone (1%)-dextrose (2%)
466 (YPD) medium supplemented with 2% agar and 200 µg ml-1 of hygromycin B (HYG) was used for colony
467 selection after biolistic transformation. Transformants were screened by PCR for intended mutations
468 and gene expression was confirmed by western blot. Plasmids and oligonucleotides used in this study
469 for strain generation are listed in **Tables S2-S3.**

470 Strains were cultivated in synthetic complete (SC) medium (MP Biomedicals) at 30°C. Media was
471 supplemented with indicated concentrations of $CuSO_4$ or the Cu^+ chelator bathocuproine disulfonate
472 (BCS) to induce Cu sufficiency or deficiency, respectively.

473 Growth phenotype analysis was performed as previously described [28, 58]. Melanization assays
474 were performed on L-3,4-dihydroxyphenylalanine (L-DOPA) media (7.6 mM L-asparagine monohydrate,
475 5.6 mM glucose, 22 mM KH_2PO_4, 1 mM MgSO4 heptahydrate, 0.5 mM L-DOPA, 0.3 µM thiamine-HCl, 20
476 nM biotin, pH 5.6) as previously described [28, 58]. L-DOPA plates were incubated at 30°C for 3 days.

477 **Trichloroacetic acid (TCA)-based protein precipitation and western blotting**

478 *Cn* cultures grown overnight for 18h in synthetic complete (SC) medium (MP Biomedicals) were
479 diluted to OD_{600} 0.5 and incubated for 2 h at 30°C in SC. Cu stress was then induced by the addition of
480 either 1 mM BCS or 1 mM $CuSO_4$, and cultures were incubated for 3 h at 30°C. TCA-precipitated protein
481 extracts were generated as previously described [59]. Precipitated proteins were solubilized in alkylating
482 buffer (0.1 M Tris pH 8.3, 1 mM EDTA, 1% SDS) for 10 min at 65°C. Crude TCA extracts were used in all
483 experiments. Prior to analysis, indicated amounts of the crude TCA extract were treated with 1x SDS-
484 loading buffer (Biorad) and boiled for 10 min at 95°C. Protein samples were run on a 7.5% TGX Mini
485 polyacrylamide gel (Biorad) using SDS running buffer (Biorad) for 35 to 40 min at 200 V. Then, proteins
486 were blotted on nitrocellulose using the Transblot Turbo system (Biorad) at the high molecular weight
487 blotting setting. Cuf1-FLAG protein levels were analyzed using a monoclonal Anti-FLAG M2-Peroxidase
488 antibody (1:5000 dilution) (Sigma, αFLAG-HRP) using a rabbit anti-β-tubulin at 1:500 dilution in 5% milk
489 + TBS-T and 0.02% sodium azide (abcam, ab15568) combined with an anti-rabbit-HRP in a dilution of
490 1:4000 (GE Healthcare) as loading control. Blots were blocked with 5% Milk in TBS-T and washed 3x for
491 15 min with TBS-T after each antibody incubation. Primary antibodies were incubated overnight at 4°C,
492 the FLAG-HRP conjugate as well as secondary antibodies were incubated for 1 h at RT. Proteins were
493 detected by chemiluminescence using the SuperSignal West Pico substrate (Thermo Fisher Scientific).

494

495 **RNA isolation and qRT-PCR**

496 For transcript analysis during high versus low Cu stress, overnight cultures (~18h) incubated in
497 synthetic complete (SC) medium (MP Biomedicals) were diluted to OD_{600} 0.5, grown for 2 h at 30°C in SC
498 medium. Cu stress was then induced by the addition of either 1 mM BCS or 1mM $CuSO_4$ and cultures
499 were grown for 3 h at 30°C.

500 For transcript analysis in melanin inducing conditions, overnight cultures incubated in SC
501 medium were diluted to OD_{600} 0.5 and incubated for 3h at 30°C in L-DOPA medium supplemented with
502 either 10 µM BCS or 10 µM $CuSO_4$.

503 RNA extraction and cDNA analysis was performed as described previously [28]. For transcript
504 analysis via qRT-PCR, cDNA was diluted 1:5 in RNase-free water and mixed with the PowerUP SYBR
505 Green Master mix (Applied Biosystems) per protocol instruction and analyzed on a QuantStudio 6 Flex
506 (Applied Biosystems). The oligonucleotides used for transcript analysis are listed in **Table S3.** Cycle
507 threshold (C_T) values were calculated using the QuantStudio 6 Flex and gene expression values were
508 normalized to *GAPDH*. Expression fold changes were calculated using the $\Delta\Delta C_T$ method. For all transcript
509 analysis a minimum of 4 independent biological replicates were analyzed.

510

511 **Chromatin immunoprecipitation followed by quantitative PCR analysis (ChIP-PCR)**

512 Overnight cultures (~18h) incubated in SC medium were diluted to OD_{600} 0.2, and incubated for
513 2 h at 30°C in SC medium. Cu stress was then induced by the addition of either 1 mM BCS or 1mM $CuSO_4$
514 and cultures were grown for 2.5 h at 30°C. Crosslinking of the samples was performed in a 1%
515 formaldehyde solution for 30 min at RT. The downstream processing and ChIP were performed as
516 previously described [23] with following adaptions: Instead of sonication 5 times, with 30s ON followed
517 by 1 min OFF, samples were processed using a Bioruptor UCD200 (Diagenode) via 24 cycles of 15 s "ON "
518 followed by 15 s "OFF" at the high level to shear chromatin. Immune precipitated DNA fragments were
519 purified with a PCR clean up kit (Macherey Nagel) following manufacturer's instructions. qPCR was
520 performed with the PowerUP SYBR Green Master mix (Applied Biosystems) per protocol instructions
521 and analyzed on a QuantStudio 6 Flex (Applied Biosystems) using oligonucleotides listed in **Table S3**. For
522 quantification, the C_T from each input was subtracted from the C_T from the target gene obtained for the
523 Cuf1–FLAG strain ($\Delta C_{T\ target}$) or the negative control (WT strain, no FLAG-tagged Cuf1, $\Delta C_{T\ control}$). Then,

524 the Δ $C_{T\ control}$ was subtracted from the $\Delta C_{T\ target}$ to give a $\Delta\Delta$ C_T value. For each gene promoter, Cuf1
525 enrichment was calculated as the inverse log of $\Delta\Delta$ C_T base 2 ($2^{\Delta\Delta Ct}$). Cuf1-FLAG enrichment at the
526 tubulin promoter was used for normalization.
527
528 **Disc diffusion assay**
529 To measure menadione-induced ROS stress sensitivity, SC overnight cultures (~18h) of indicated
530 *Cn* strains were diluted 1:500 in SC medium, and 500 µL cell suspension spread onto SC plates or SC
531 plates supplemented with indicated amounts of BCS or $CuSO_4$. Inoculated plates were dried for 45 min
532 at RT. Filter discs were spotted with 15 µL of the indicated concentrations of menadione (dissolved in
533 ethanol) and set in quadrants around the plates. Plates were incubated at 30 °C for 3 to 4 days.
534
535 **Protein extraction and Sod activity assay**
536 For Sod activity analysis, *Cn* overnight cultures (~18h) incubated in synthetic SC medium were diluted to
537 OD_{600} 0.1 in SC medium or SC medium supplemented with either 250 µM BCS or 50 µM or 100 µM
538 $CuSO_4$. Cultures were incubated for 24 h at 30°C. For protein extraction, cells were pelleted (1 min,
539 11000xg, 4°C), washed 1x with cold Lysis buffer (10 mM sodium phosphate, 50 mM NaCl, 0.1% triton X-
540 100, 10% glycerol pH 7.8 made in chelex-treated H_2O) and resuspended in 350 µL of cold lysis buffer + 1x
541 Protease Inhibitor cocktail (ROCHE) and PMSF. Cells were lysed with a Bead Ruptor 12 (Omni
542 international) using 6 cycles of 60s "ON" and 90s "OFF", 5.5 speed at 4°C. Cell lysates were clarified for
543 15 min at 21000xg at 4°C and the clarified lysate was transferred into a 1.5 mL reaction tube. Total
544 protein levels were measured using a BCA kit (Thermo Fisher Scientific) according to manufacturer's
545 instruction. Lysates were diluted to a concentration of 75 µg protein in 25 µL native sample buffer (Bio-
546 Rad, catalog #1610738) and lysis buffer to a final volume of 50 µL. Diluted lysates at a volume of 20 µL
547 were loaded onto a 10% mini-PROTEAN TGX precast protein gel (Bio-Rad, catalog #4561033).

548 Electrophoresis was performed in 1X tris glycine running buffer at 200 V and 4°C for approximately 1 h.
549 Gels were then incubated at RT in the dark for 1 h in 50 mL NBT staining solution (50 mM potassium
550 phosphate, 30 µM riboflavin, 0.48 mM nitro blue tetrazolium chloride, pH 7.8) while shaking at 60 rpm.
551 NBT staining solution was decanted and gels were soaked in diH_2O in the light for approximately 30 min
552 before imaging on an iBright 1500 FL Imager (Thermo Fisher Scientific).
553
554 **Infection experiments**
555 We used the murine inhalation model of cryptococcosis [59] to assess fungal survival and host
556 response after lung infection. For each strain, 5 female A/J mice were used. Mice were anesthetized by
557 isoflurane inhalation and intranasally inoculated with 1×10^5 fungal cells of PBS-washed overnight
558 cultures (~18h) of indicated strains in SC. Mice were sacrificed at 14 days post infection and the mouse
559 lung harvested, weighed, and homogenized in cold PBS. Colony forming units (CFU) were calculated by
560 quantitative culture and are represented as CFU/lung. For Histopathology at 14 days post infection, mice
561 were sacrificed using a lethal dose of pentobarbital sodium, and lungs were fixed via intratracheal
562 instillation of neutral buffered formalin under gravity flow [60]. Fixed lungs were submitted to the
563 Immunohistopathology Core at Duke University for paraffin embedding and staining with hematoxylin
564 and eosin. A pathologist assessed the distribution of the yeast cells and the immune response in a
565 blinded analysis.
566
567 **Statistical analysis**
568 All data error bars represent standard errors of the means (SEM) of results from a number of
569 biological replicates (N), as indicated in figure legends. Prior to statistical analysis, data from all
570 experiments was $\log_2$ transformed for comparison of proportions. Statistical analysis was conducted

571 using the GraphPad Prism software v9. The statistical tests used in each experiment and their results
572 (i.e., p values) are indicated in figure legends. Asterisks in figures correspond to statistical significance as
573 follows: ****, $P < 0.0001$; ***, $P = 0.0001$ to $P < 0.001$; **, $P = 0.001$ to $P < 0.01$; *, $P = 0.01$ to $P < 0.05$;
574 ns (not significant), $P > 0.05$.
575

576 ## Acknowledgements

577 We thank the Duke Immunohistopathology Core for preparation and staining of the infected lung tissue.
578 We thank Dr. Connie Nichols for the careful reading of the manuscript. C.D.J. and K.J.F. acknowledge
579 support by the National Institute of General Medical Sciences of the National Institutes of Health (NIH)
580 under award number R01GM145035. This work was further supported by an NIH grant R01GM041840
581 (J.A.A. and C.P.) and by Duke University School of Medicine Bridge Funding 4532750.

582

583 ## FIGURE LEGENDS

584

585 **Figure 1: The Cuf1-FLAG ΔAce1 mutant protein is produced to WT levels but fails to restore growth**
586 **during high Cu stress.**

587 **(A-B)** Schematic representation of the *Cn*Cuf1 N- and C-terminal domains and the Cuf1-FLAG WT and
588 ΔAce1 mutant proteins. The first and last residues of each domain are indicated. The N-terminal domain
589 is shown in grey; the C-terminal domain is shown in pale yellow. The N-terminal DNA binding motif,
590 which contains the conserved KGRP DNA binding motif, is highlighted in orange. The Ace1-like cysteine-
591 rich region is indicated via blue box, and the Mac1-like regions are indicated by an orange box. The
592 sequence of the identified cysteine-rich regions is indicated for each region as well as (B) the cysteine-
593 to-alanine mutations performed to generate the ΔAce1 mutant protein. **(C)** Cuf1-FLAG WT and ΔAce1
594 mutant protein expression assessed by western blot analysis. The *CUF1-FLAG* WT or the *CUF1-FLAG*

595 ΔAce1 mutant strains were incubated in SC medium supplemented with either 1mM $CuSO_4$ or 1 mM BCS
596 at a starting OD_{600} of 0.5 for 3 h at 30°C. A TCA based protein extraction was performed. 25 µL of crude
597 TCA extract was analyzed per lane with the α FLAG-HRP conjugate. The α β-Tubulin (anti-β-tubulin)
598 antibody was used as a loading control. **(D)** Growth analysis in the presence of high and low Cu stress.
599 Five-fold serial dilutions of cell suspensions for each strain were spotted onto SC medium plates. To
600 induce low Cu stress, the SC medium was supplemented with 0.5 or 1 mM BCS. To induce varying
601 degrees of high Cu stress, the SC medium was supplemented with either 0.02, 0.05, 0.1, 0.25 or 1 mM
602 $CuSO_4$. Plates were incubated at 30°C for 3 d. Two independent *CUF1-FLAG Δ*Ace1 mutant strains were
603 analyzed. As Cu stress controls, the Cu import mutant *ctr1*Δ *ctr4*Δ and the Cu detoxification mutant
604 *mt1*Δ *mt2*Δ were included in the growth analysis.

605

606 **Figure 2: Mutation of the Ace1-like Cys-rich region renders Cuf1 unable to bind to and activate high**
607 **Cu regulated genes.**

608 **(A-B)** Transcript abundance of the high Cu-regulated *MT1* and *CTR4* genes (A) and the low Cu-regulated
609 *CTR4* and *CBI1* genes (B). Indicated strains were diluted to OD_{600} of 0.5 and incubated for 2 h at 30°C in
610 SC medium. Cu stress was induced by the addition of either 1 mM BCS or 1mM $CuSO_4$ and cultures were
611 incubated for 3 h at 30°C. Transcript abundance for each indicated gene was assessed by quantitative
612 real-time PCR (qPCR), and the log_2 fold change of transcripts was calculated using the ΔΔ C_T method in
613 high Cu stress versus low Cu stress (A) or low Cu stress versus high Cu stress (B). Transcript levels were
614 normalized to *GAPDH*. Shown is the mean +/- SEM of 4 biological replicates. Statistical analysis was
615 performed using one-way ANOVA. **(C-D)** Cuf1-FLAG promoter binding at high Cu stress (A) or low Cu
616 stress (B). Indicated strains were diluted to OD_{600} of 0.25 and incubated for 2 h at 30°C in SC medium. Cu
617 stress was induced by the addition of either 1 mM BCS or 1mM $CuSO_4$, and cultures were incubated for

618 2.5 h at 30°C prior to crosslinking. Promoter binding to the target promoters was analyzed via chromatin
619 immunoprecipitation followed by quantitative PCR (ChIP-PCR). Fold enrichment was calculated by
620 comparison of target promoter abundance in the FLAG-tagged strains to the promoter abundance in the
621 non-FLAG tagged, WT strain. The mean +/- SEM of 3 biological replicates is shown. A two-tailed t-test
622 was performed as statistical analysis.
623

624 **Figure 3: Cuf1 Ace1-like Cys rich region is essential for *LAC1* regulation in response to excess copper.**

625 **(A)** Schematic summary of the role of copper and Cuf1 for Lac1 activity and melanin production during
626 both Cu limitation and Cu excess. In the absence of Cuf1-induction of Cu-import genes during Cu
627 limitation, melanin production by the Cu-dependent laccase Lac1 is impaired. Cuf1 is also required for
628 expression of the *LAC1* gene during Cu excess. Images were designed using Biorender. **(B)** Melanization
629 during Cu limitation (10 µM BCS) and in presence of exogenous copper (10 µM $CuSO_4$). Indicated strains
630 were grown for 18h in SC at 30°C, diluted to OD_{600} of 2.5 and spotted onto L-DOPA agar plates with
631 indicated supplementation. L-DOPA plates were incubated for 3 d at 30°C. Melanin production is
632 demonstrated by colony pigmentation **(C-D)** *LAC1* (C) and *CTR4* (D) transcript abundance in melanin-
633 inducing conditions. Indicated strains were diluted to OD_{600} of 0.5 in liquid L-DOPA medium
634 supplemented with either 10 µM BCS or 10 µM $CuSO_4$ and grown for 3 h at 30°C. Relative transcript
635 abundance for *LAC1* (C) or *CTR4* (D) was assessed by quantitative RT-PCR and normalized to WT
636 transcript levels via the $\Delta\Delta C_T$ method. The data is presented as the mean +/- SEM of the Log_2 fold change
637 of 3 biological replicates. Statistical analysis was performed using a one-way ANOVA.

638

639 **Figure 4: Cuf1 Ace1-like Cys rich region is required for superoxide dismutase (Sod)-dependent ROS**
640 **detoxification during high Cu stress.**

641 **(A)** Schematic summary of the role of copper and Cuf1 for Sod protein regulation during Cu limitation
642 and excess. Cu, Zn-containing Sod1 is the major cytosolic Sod in Cu sufficiency and excess. The Mn-
643 dependent mitochondrial Sod2 assumes the majority of cytosolic Sod function in Cu limitation. Images
644 were designed using Biorender. **(B-C)** Disc diffusion assay to test cellular superoxide sensitivities.
645 Indicated strains were inoculated on SC agar plates supplemented with indicated amounts of BCS or
646 $CuSO_4$. Cells were challenged with increasing concentrations of the superoxide generator menadione on
647 filter discs as outlined (B) for 3 days at 30 °C (C). **(D)** In-gel SOD activity assays from whole cell extracts of
648 indicated strains. For Cu stress induction, strains were incubated in SC medium supplemented with
649 indicated amounts of BCS or $CuSO_4$ for 24 h at 30°C. Whole cell extracts were generated, separated by
650 native PAGE, and stained for SOD activity using nitroblue tetrazolium (NBT) staining solution. **(E)**
651 Transcript abundance of the *SOD1* gene during high Cu and low Cu stress. Indicated strains were diluted
652 to OD_{600} 0.5, and incubated for 2 h at 30°C in SC medium. Cu stress was induced by the addition of either
653 1 mM BCS or 1mM $CuSO_4$ and cultures were incubated for 3 h at 30°C. Relative transcript abundance for
654 *SOD1* was assessed by quantitative RT-PCR and normalized to WT transcript levels using the $\Delta\Delta C_T$
655 method. The data is presented as the mean +/- SEM of the Log_2 fold change of 3 biological replicates and
656 statistical analysis was performed using a one-way ANOVA.

657

658 **Figure 5: Effects of Cuf1 high Cu stress regulation on survival and immune recognition in the infected**
659 **lung.**

660 **(A-C)** Lung fungal burden 14 days postinfection. Female A/J mice (5 mice per strain) were infected by
661 inhalation with 10^5 cells of the indicated strains. Mice were sacrificed 14 d postinfection and their lungs
662 harvested. Lung lysates were assessed by quantitative culture (A), lung wet weight (B) and macroscopic
663 lung abnormalities (C). (A-B) Data were plotted, and an unpaired t-test was performed using GraphPad
664 Prism (B only). (C) Foci are indicated with white arrows. **(D)** Histopathology analysis of infected murine
665 lungs 14 days post infection. Mice were infected as described above. Mice were sacrificed and lungs
666 were fixed via intratracheal instillation of neutral buffered formalin under gravity flow. Hematoxylin and
667 eosin staining were used to visualize microscopic lung pathology. Yeast enriched foci of inflammation
668 are highlighted by a black arrowhead. The length of the black bar represents 250 µm.

669

670 ## SUPPLEMENTAL

671 **Supplemental Figure S1:**

672 **(A)** *CDA2* and *CFO1* transcript abundance at high end low Cu stress. Indicated strains were diluted to
673 OD_{600} of 0.5 and, incubated for 2 h at 30°C in SC medium. Cu stress was induced by the addition of either
674 1 mM BCS or 1mM $CuSO_4$ and cultures were incubated for 3 h at 30°C. Relative transcript abundance
675 was assessed by quantitative RT-PCR and normalized to WT transcript levels via the $\Delta\Delta C_T$ method. The
676 data is presented as the mean +/- SEM of the Log_2 fold change of 4 biological replicates. A one-way
677 ANOVA was performed. **(B-C)** Cuf1-FLAG promoter binding at high Cu stress (B) or low Cu stress (C).
678 Indicated strains were diluted to OD_{600} of 0.25 and incubated for 2 h at 30°C in SC medium. Cu stress was
679 induced by the addition of either 1 mM BCS or 1mM $CuSO_4$, and cultures were incubated for 2.5 h at
680 30°C prior to crosslinking. Promoter binding was analyzed via chromatin immunoprecipitation followed
681 by quantitative PCR (ChIP-PCR). Fold enrichment was calculated by comparison of promoter abundance

682 in the Cuf1-FLAG strain to the promoter abundance in the WT strain. The presented data show the mean

683 +/- SEM of 3 biological replicates.

684

685 **Supplemental Table S1: Strains used in this study.**

686 **Supplemental Table S2: Plasmids used in this study.**

687 **Supplemental Table S3: Oligonucleotides used in this study.**

688

689

690 **References**

691 1. Maret W. The Metals in the Biological Periodic System of the Elements: Concepts and
692 Conjectures. *International journal of molecular sciences*. 2016;17(1). Epub 2016/01/08. doi:
693 10.3390/ijms17010066.

694 2. Smith AD, Logeman BL, Thiele DJ. Copper Acquisition and Utilization in Fungi. *Annual review of*
695 *microbiology*. 2017;71:597-623. Epub 2017/09/10. doi: 10.1146/annurev-micro-030117-020444.

696 3. Halliwell B, Gutteridge JM. The importance of free radicals and catalytic metal ions in human
697 diseases. *Molecular aspects of medicine*. 1985;8(2):89-193. Epub 1985/01/01. doi: 10.1016/0098-
698 2997(85)90001-9.

699 4. Giachino A, Waldron KJ. Copper tolerance in bacteria requires the activation of multiple
700 accessory pathways. 2020;114(3):377-90. doi: https://doi.org/10.1111/mmi.14522.

701 5. Robison ATR, Sturrock GR, Zaengle-Barone JM, Wiebelhaus N, Dharani A, Williams IG, *et al.*
702 Analysis of copper-induced protein precipitation across the *E. coli* proteome. *Metallomics : integrated*
703 *biometal science*. 2023;15(1). Epub 2022/12/23. doi: 10.1093/mtomcs/mfac098.

704 6. Zuily L, Lahrach N, Fassler R, Genest O, Faller P, Sénèque O, *et al.* Copper Induces Protein
705 Aggregation, a Toxic Process Compensated by Molecular Chaperones. *mBio*. 2022;13(2):e0325121. Epub
706 2022/03/16. doi: 10.1128/mbio.03251-21.

707 7. Macomber L, Imlay JA. The iron-sulfur clusters of dehydratases are primary intracellular targets
708 of copper toxicity. *Proceedings of the National Academy of Sciences of the United States of America*.
709 2009;106(20):8344-9. Epub 2009/05/07. doi: 10.1073/pnas.0812808106.

710 8. Imlay JA. The mismetallation of enzymes during oxidative stress. *The Journal of biological*
711 *chemistry*. 2014;289(41):28121-8. Epub 2014/08/28. doi: 10.1074/jbc.R114.588814.

712 9. Merchant SS, Schmollinger S, Strenkert D, Moseley JL, Blaby-Haas CE. From economy to luxury:
713 Copper homeostasis in *Chlamydomonas* and other algae. *Biochimica et biophysica acta Molecular cell*
714 *research*. 2020;1867(11):118822. Epub 2020/08/18. doi: 10.1016/j.bbamcr.2020.118822.
715 10. Li CX, Gleason JE, Zhang SX, Bruno VM, Cormack BP, Culotta VC. *Candida albicans* adapts to host
716 copper during infection by swapping metal cofactors for superoxide dismutase. *Proceedings of the*
717 *National Academy of Sciences of the United States of America*. 2015;112(38):E5336-42. Epub
718 2015/09/10. doi: 10.1073/pnas.1513447112.
719 11. Smith AD, Garcia-Santamarina S, Ralle M, Loiselle DR, Haystead TA, Thiele DJ. Transcription
720 factor-driven alternative localization of *Cryptococcus neoformans* superoxide dismutase. *The Journal of*
721 *biological chemistry*. 2021;296:100391. Epub 2021/02/11. doi: 10.1016/j.jbc.2021.100391.
722 12. Ray SC, Rappleye CA. Mac1-Dependent Copper Sensing Promotes *Histoplasma* Adaptation to the
723 Phagosome during Adaptive Immunity. 2022;13(2):e03773-21. doi: doi:10.1128/mbio.03773-21.
724 13. Mohamed SH, Fu MS, Hain S, Alselami A, Vanhoffelen E, Li Y, *et al.* Microglia are not protective
725 against *cryptococcal* meningitis. *Nature communications*. 2023;14(1):7202. Epub 2023/11/08. doi:
726 10.1038/s41467-023-43061-0.
727 14. García-Santamarina S, Thiele DJ. Copper at the Fungal Pathogen-Host Axis. *The Journal of*
728 *biological chemistry.* 2015;290(31):18945-53. Epub 2015/06/10. doi: 10.1074/jbc.R115.649129.
729 15. Murdoch CC, Skaar EP. Nutritional immunity: the battle for nutrient metals at the host–
730 pathogen interface. *Nature Reviews Microbiology*. 2022;20(11):657-70. doi: 10.1038/s41579-022-00745-
731 6.
732 16. Besold Angelique N, Gilston Benjamin A, Radin Jana N, Ramsoomair C, Culbertson Edward M, Li
733 Cissy X, *et al.* Role of Calprotectin in Withholding Zinc and Copper from *Candida albicans*. *Infection and*
734 *Immunity*. 2018;86(2):10.1128/iai.00779-17. doi: 10.1128/iai.00779-17.

735 17. Garg R, David MS, Yang S, Culotta VC. Metals at the Host–Fungal Pathogen Battleground.
736 2024;78(Volume 78, 2024):23-38. doi: https://doi.org/10.1146/annurev-micro-041222-023745.
737 18. White C, Lee J, Kambe T, Fritsche K, Petris MJ. A role for the ATP7A copper-transporting ATPase
738 in macrophage bactericidal activity. *The Journal of biological chemistry*. 2009;284(49):33949-56. Epub
739 2009/10/08. doi: 10.1074/jbc.M109.070201.
740 19. Rajasingham R, Smith RM, Park BJ, Jarvis JN, Govender NP, Chiller TM, *et al.* Global burden of
741 disease of HIV-associated *cryptococcal* meningitis: an updated analysis. *The Lancet Infectious diseases*.
742 2017;17(8):873-81. Epub 2017/05/10. doi: 10.1016/s1473-3099(17)30243-8.
743 20. Heitman J, Kozel TR, Kwon-Chung KJ, Perfect JR, Casadevall A. *Cryptococcus* : from human
744 pathogen to model yeast. *ASM Press*; 2011. Available from:
745 http://www.asmscience.org/content/book/10.1128/9781555816858.
746 21. Ding C, Festa RA, Chen YL, Espart A, Palacios Ò, Espín J, *et al. Cryptococcus neoformans* copper
747 detoxification machinery is critical for fungal virulence. *Cell host & microbe*. 2013;13(3):265-76. Epub
748 2013/03/19. doi: 10.1016/j.chom.2013.02.002.
749 22. Sun TS, Ju X, Gao HL, Wang T, Thiele DJ, Li JY, *et al.* Reciprocal functions of *Cryptococcus*
750 *neoformans* copper homeostasis machinery during pulmonary infection and meningoencephalitis.
751 *Nature communications*. 2014;5:5550. Epub 2014/11/25. doi: 10.1038/ncomms6550.
752 23. Garcia-Santamarina S, Festa RA, Smith AD, Yu CH, Probst C, Ding C, *et al.* Genome-wide analysis
753 of the regulation of Cu metabolism in *Cryptococcus neoformans*. *Molecular microbiology*.
754 2018;108(5):473-94. Epub 2018/04/03. doi: 10.1111/mmi.13960.
755 24. Garcia-Santamarina S, Uzarska MA, Festa RA, Lill R, Thiele DJ. *Cryptococcus neoformans* Iron-
756 Sulfur Protein Biogenesis Machinery Is a Novel Layer of Protection against Cu Stress. *mBio*. 2017;8(5).
757 Epub 2017/11/02. doi: 10.1128/mBio.01742-17.

758 25. Do E, Park S, Li MH, Wang JM, Ding C, Kronstad JW, *et al*. The mitochondrial ABC transporter
759 Atm1 plays a role in iron metabolism and virulence in the human fungal pathogen *Cryptococcus*
760 *neoformans*. *Medical mycology*. 2018;56(4):458-68. Epub 2018/02/09. doi: 10.1093/mmy/myx073.
761 26. Cox GM, Harrison TS, McDade HC, Taborda CP, Heinrich G, Casadevall A, *et al.* Superoxide
762 dismutase influences the virulence of *Cryptococcus neoformans* by affecting growth within
763 macrophages. *Infect Immun*. 2003;71(1):173-80. Epub 2002/12/24. doi: 10.1128/iai.71.1.173-180.2003.
764 27. Garcia-Santamarina S, Probst C, Festa RA, Ding C, Smith AD, Conklin SE, *et al.* A lytic
765 polysaccharide monooxygenase-like protein functions in fungal copper import and meningitis. *Nature*
766 *Chemical Biology*. 2020;16(3):337-44. doi: 10.1038/s41589-019-0437-9.
767 28. Probst C, Garcia-Santamarina S, Brooks JT, Van Der Kloet I, Baars O, Ralle M, *et al.* Interactions
768 between copper homeostasis and the fungal cell wall affect copper stress resistance. *PLoS pathogens*.
769 2022;18(6):e1010195. Epub 2022/06/24. doi: 10.1371/journal.ppat.1010195.
770 29. Thiele DJ. *ACE1* regulates expression of the *Saccharomyces cerevisiae* metallothionein gene.
771 *Molecular and cellular biology*. 1988;8(7):2745-52. Epub 1988/07/01. doi: 10.1128/mcb.8.7.2745-
772 2752.1988.
773 30. Culotta VC, Hsu T, Hu S, Fürst P, Hamer D. Copper and the *ACE1* regulatory protein reversibly
774 induce yeast metallothionein gene transcription in a mouse extract. *Proceedings of the National*
775 *Academy of Sciences of the United States of America*. 1989;86(21):8377-81. Epub 1989/11/01. doi:
776 10.1073/pnas.86.21.8377.
777 31. Jungmann J, Reins HA, Lee J, Romeo A, Hassett R, Kosman D, *et al. MAC1*, a nuclear regulatory
778 protein related to Cu-dependent transcription factors is involved in Cu/Fe utilization and stress
779 resistance in yeast. *The EMBO journal*. 1993;12(13):5051-6. Epub 1993/12/15. doi: 10.1002/j.1460-
780 2075.1993.tb06198.x.

781 32. Waterman SR, Hacham M, Hu G, Zhu X, Park YD, Shin S, *et al.* Role of a CUF1/CTR4 copper
782 regulatory axis in the virulence of *Cryptococcus neoformans*. *The Journal of clinical investigation*.
783 2007;117(3):794-802. Epub 2007/02/10. doi: 10.1172/jci30006.
784 33. Szczypka MS, Thiele DJ. A cysteine-rich nuclear protein activates yeast metallothionein gene
785 transcription. *Molecular and cellular biology*. 1989;9(2):421-9. Epub 1989/02/01. doi:
786 10.1128/mcb.9.2.421-429.1989.
787 34. Graden JA, Posewitz MC, Simon JR, George GN, Pickering IJ, Winge DR. Presence of a copper(I)-
788 thiolate regulatory domain in the copper-activated transcription factor Amt1. *Biochemistry*.
789 1996;35(46):14583-9. Epub 1996/11/19. doi: 10.1021/bi961642v.
790 35. Koch KA, Thiele DJ. Autoactivation by a *Candida glabrata* copper metalloregulatory transcription
791 factor requires critical minor groove interactions. *Molecular and cellular biology*. 1996;16(2):724-34.
792 Epub 1996/02/01. doi: 10.1128/mcb.16.2.724.
793 36. Serpe M, Joshi A, Kosman DJ. Structure-function analysis of the protein-binding domains of
794 Mac1p, a copper-dependent transcriptional activator of copper uptake in *Saccharomyces cerevisiae*. *The*
795 *Journal of biological chemistry*. 1999;274(41):29211-9. Epub 1999/10/03. doi:
796 10.1074/jbc.274.41.29211.
797 37. Fürst P, Hu S, Hackett R, Hamer D. Copper activates metallothionein gene transcription by
798 altering the conformation of a specific DNA binding protein. Cell. 1988;55(4):705-17. Epub 1988/11/18.
799 doi: 10.1016/0092-8674(88)90229-2.
800 38. Upadhya R, Lam WC, Hole CR, Parchment D, Lee CK, Specht CA, *et al. Cryptococcus neoformans*
801 Cda1 and Cda2 coordinate deacetylation of chitin during infection to control fungal virulence. *Cell*
802 *surface*. 2021;7:100066. Epub 2021/10/30. doi: 10.1016/j.tcsw.2021.100066.

803 39. Kim J, Cho Y-J, Do E, Choi J, Hu G, Cadieux B, *et al.* A defect in iron uptake enhances the
804 susceptibility of *Cryptococcus neoformans* to azole antifungal drugs. *Fungal Genetics and Biology*.
805 2012;49(11):955-66. doi: https://doi.org/10.1016/j.fgb.2012.08.006.
806 40. Camacho E, Vij R, Chrissian C, Prados-Rosales R, Gil D, O'Meally RN, *et al.* The structural unit of
807 melanin in the cell wall of the fungal pathogen *Cryptococcus neoformans*. *The Journal of biological*
808 *chemistry*. 2019;294(27):10471-89. Epub 2019/05/24. doi: 10.1074/jbc.RA119.008684.
809 41. Zhu X, Williamson PR. Role of laccase in the biology and virulence of *Cryptococcus neoformans*.
810 *FEMS Yeast Research*. 2004;5(1):1-10. doi: 10.1016/j.femsyr.2004.04.004 %J FEMS Yeast Research.
811 42. Jiang N, Sun N, Xiao D, Pan J, Wang Y, Zhu X. A copper-responsive factor gene *CUF1* is required
812 for copper induction of laccase in *Cryptococcus neoformans*. *FEMS microbiology letters*. 2009;296(1):84-
813 90. Epub 2009/05/23. doi: 10.1111/j.1574-6968.2009.01619.x.
814 43. Xue P, Hu G, Jung WH, Kronstad JW. Metals and the cell surface of *Cryptococcus neoformans*.
815 Current Opinion in Microbiology. 2023;74:102331. doi: https://doi.org/10.1016/j.mib.2023.102331.
816 44. Telzrow CL, Esher Righi S, Castro-Lopez N, Campuzano A, Brooks JT, Carney JM, *et al.* An
817 Immunogenic and Slow-Growing *Cryptococcal* Strain Induces a Chronic Granulomatous Infection in
818 Murine Lungs. *Infect Immun*. 2022;90(6):e0058021. Epub 2022/05/20. doi: 10.1128/iai.00580-21.
819 45. Cai Z, Du W, Zhang Z, Guan L, Zeng Q, Chai Y, *et al.* The transcription factor AceA is involved not
820 only in Cu but also in Zn detoxification through regulating transporters CrpA and ZrcA.
821 2018;20(10):e12864. doi: https://doi.org/10.1111/cmi.12864.
822 46. Upadhyay S, Torres G, Lin X. Laccases involved in 1,8-dihydroxynaphthalene melanin
823 biosynthesis in *Aspergillus fumigatus* are regulated by developmental factors and copper homeostasis.
824 *Eukaryotic cell.* 2013;12(12):1641-52. Epub 2013/10/15. doi: 10.1128/ec.00217-13.

825 47. Saikia S, Oliveira D, Hu G, Kronstad J. Role of ferric reductases in iron acquisition and virulence in
826 the fungal pathogen *Cryptococcus neoformans*. *Infect Immun*. 2014;82(2):839-50. Epub 2014/01/31. doi:
827 10.1128/iai.01357-13.
828 48. Ray Stephanie C, Rappleye Chad A. Mac1-Dependent Copper Sensing Promotes *Histoplasma*
829 Adaptation to the Phagosome during Adaptive Immunity. *mBio*. 2022;13(2):e03773-21. doi:
830 10.1128/mbio.03773-21.
831 49. Khemiri I, Tebbji F, Sellam A. Transcriptome Analysis Uncovers a Link Between Copper
832 Metabolism, and Both Fungal Fitness and Antifungal Sensitivity in the Opportunistic Yeast *Candida*
833 *albicans*. 2020;11. doi: 10.3389/fmicb.2020.00935.
834 50. Cai Z, Du W, Zeng Q, Long N, Dai C, Lu L. Cu-sensing transcription factor Mac1 coordinates with
835 the Ctr transporter family to regulate Cu acquisition and virulence in *Aspergillus fumigatus*. *Fungal*
836 *Genetics and Biology*. 2017;107:31-43. doi: https://doi.org/10.1016/j.fgb.2017.08.003.
837 51. Ballou ER, Wilson D. The roles of zinc and copper sensing in fungal pathogenesis. *Current*
838 *Opinion in Microbiology*. 2016;32:128-34. doi: https://doi.org/10.1016/j.mib.2016.05.013.
839 52. Moraes D, Tristão GB, Rappleye CA, Ray SC, Ribeiro-Dias F, Gomes RS, *et al.* The influence of a
840 copper efflux pump in *Histoplasma capsulatum* virulence. *The FEBS journal*. 2024;291(4):744-60. Epub
841 2023/11/11. doi: 10.1111/febs.16999.
842 53. Ost KS, Esher SK, Leopold Wager CM, Walker L, Wagener J, Munro C, *et al.* Rim Pathway-
843 Mediated Alterations in the Fungal Cell Wall Influence Immune Recognition and Inflammation. *mBio*.
844 2017;8(1). doi: https://doi.org/10.1128/mbio.02290-16.
845 54. Esher SK, Ost KS, Kohlbrenner MA, Pianalto KM, Telzrow CL, Campuzano A, *et al.* Defects in
846 intracellular trafficking of fungal cell wall synthases lead to aberrant host immune recognition. *PLoS*
847 *pathogens*. 2018;14(6):e1007126. Epub 2018/06/05. doi: 10.1371/journal.ppat.1007126.

848 55. Hole CR, Lam WC, Upadhya R, Lodge JK. *Cryptococcus neoformans* Chitin Synthase 3 Plays a
849 Critical Role in Dampening Host Inflammatory Responses. 2020;11(1):10.1128/mbio.03373-19. doi:
850 doi:10.1128/mbio.03373-19.
851 56. Upadhya R, Lam WC, Hole CR, Vasselli JG, Lodge JK. Cell wall composition in *Cryptococcus*
852 *neoformans* is media dependent and alters host response, inducing protective immunity. *Frontiers in*
853 *fungal biology*. 2023;4. Epub 2023/08/04. doi: 10.3389/ffunb.2023.1183291.
854 57. Toffaletti DL, Rude TH, Johnston SA, Durack DT, Perfect JR. Gene transfer in *Cryptococcus*
855 *neoformans* by use of biolistic delivery of DNA. *Journal of Bacteriology*. 1993;175(5):1405-11. doi:
856 10.1128/jb.175.5.1405-1411.1993.
857 58. Upadhya R, Probst C, Alspaugh JA, Lodge JK. Measuring Stress Phenotypes in *Cryptococcus*
858 *neoformans*. *Methods in molecular biology*. 2024;2775:277-303. Epub 2024/05/17. doi: 10.1007/978-1-
859 0716-3722-7_19. PubMed PMID: 38758325.
860 59. Probst C, Hallas-Møller M, Ipsen J, Brooks JT, Andersen K, Haon M, *et al.* A fungal lytic
861 polysaccharide monooxygenase is required for cell wall integrity, thermotolerance, and virulence of the
862 fungal human pathogen *Cryptococcus neoformans*. *PLoS pathogens*. 2023;19(4):e1010946. Epub
863 2023/04/26. doi: 10.1371/journal.ppat.1010946.
864 60. Hsia CC, Hyde DM, Ochs M, Weibel ER. An official research policy statement of the American
865 Thoracic Society/European Respiratory Society: standards for quantitative assessment of lung structure.
866 *American journal of respiratory and critical care medicine*. 2010;181(4):394-418. Epub 2010/02/05. doi:
867 10.1164/rccm.200809-1522ST.

868

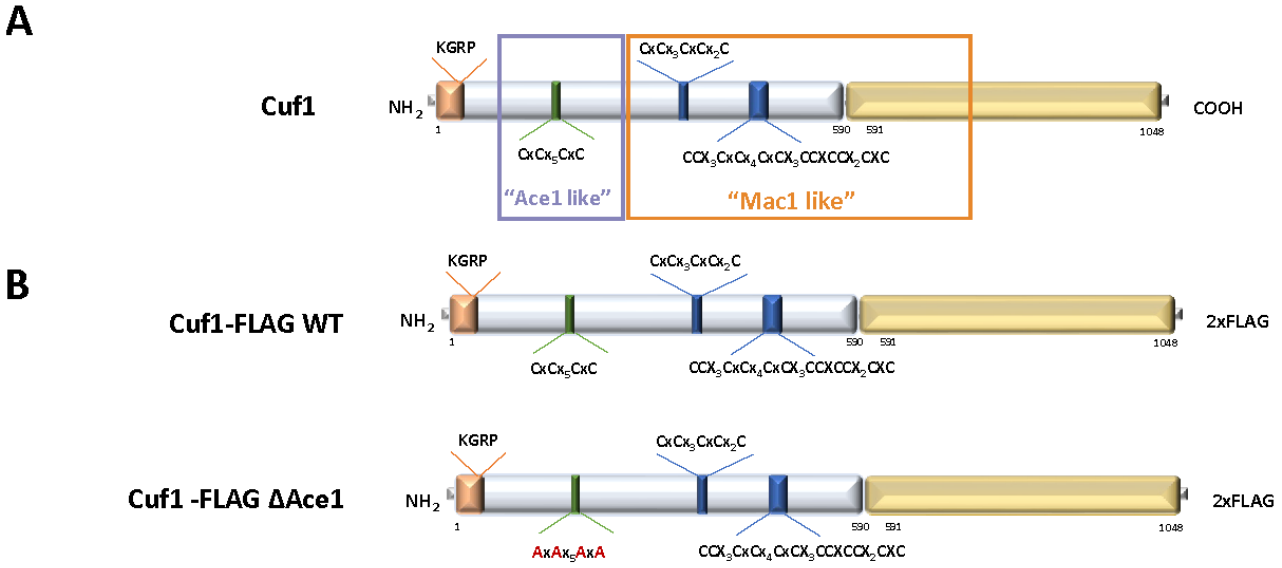
A
Cuf1
KGRP
NH2
COOH
CxCx5CxC
CxCx3CxCx2C
CCX3CxCx4CxCX3CCXCCX2CXC
"Ace1 like"
"Mac1 like"
B
Cuf1-FLAG WT
2xFLAG
Cuf1 -FLAG ΔAce1
AxAx5AxA

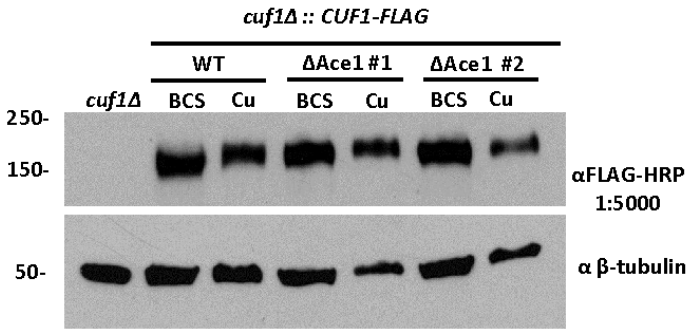
C
cuf1Δ :: CUF1-FLAG
WT
ΔAce1 #1
ΔAce1 #2
cuf1Δ
BCS
Cu
250-
150-
50-
αFLAG-HRP
1:5000
α β-tubulin

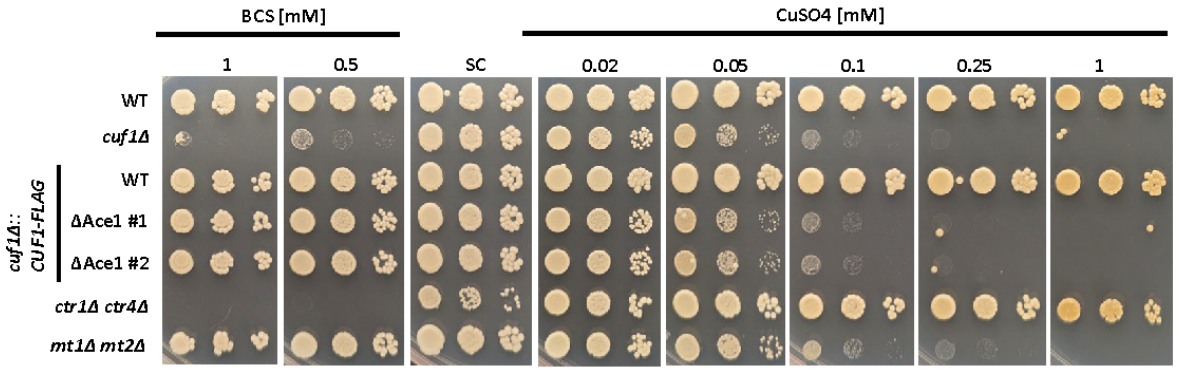
D
BCS [mM]
CuSO4 [mM]
1
0.5
SC
0.02
0.05
0.1
0.25
1
WT
cuf1Δ
cuf1Δ::
CUF1-FLAG
ΔAce1 #1
ΔAce1 #2
ctr1Δ ctr4Δ
mt1Δ mt2Δ

Figure 1

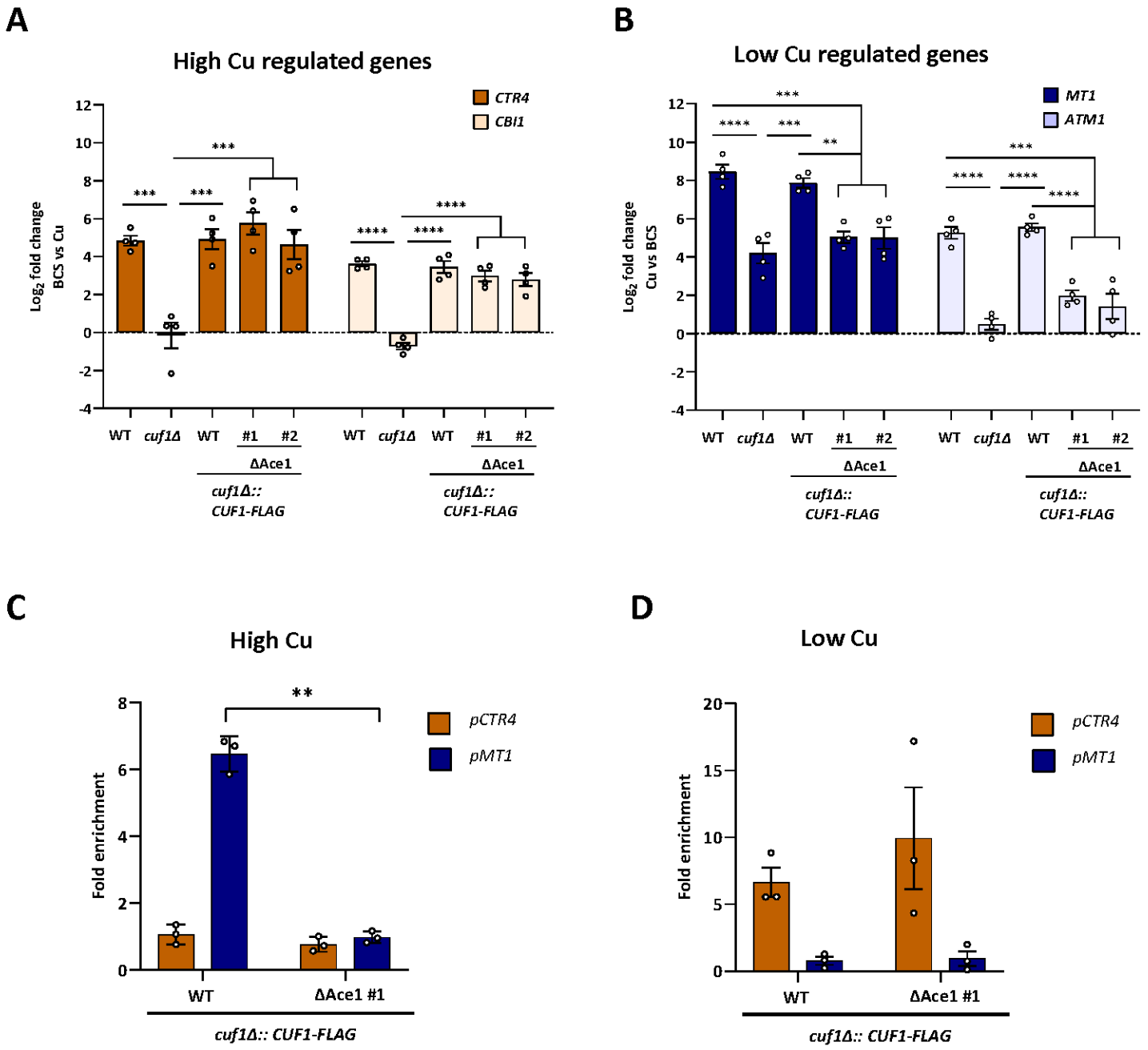
A
High Cu regulated genes
CTR4
CBI1
Log2 fold change BCS vs Cu
WT
cuf1Δ
WT
#1
#2
ΔAce1
cuf1Δ:: CUF1-FLAG
B
Low Cu regulated genes
MT1
ATM1
Log2 fold change Cu vs BCS
C
High Cu
pCTR4
pMT1
Fold enrichment
WT
ΔAce1 #1
cuf1Δ:: CUF1-FLAG
D
Low Cu

Figure 2

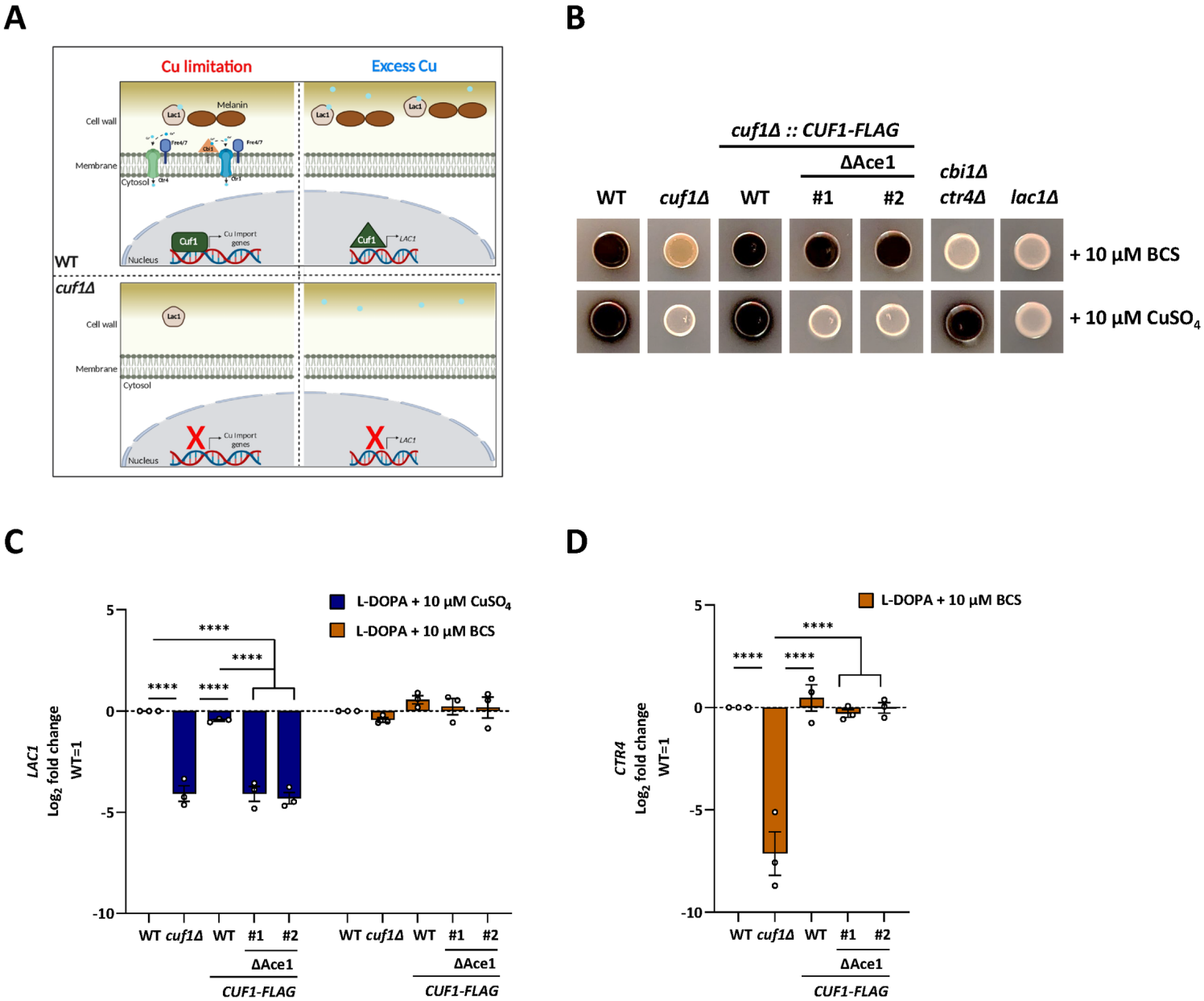
A
Cu limitation
Excess Cu
Cell wall
Membrane
Cytosol
Melanin
Lac1
Fre4/7
Ctr1
Ctr4
Cuf1
Cu import genes
LAC1
Nucleus
WT
cuf1Δ
B
cuf1Δ :: CUF1-FLAG
ΔAce1
cbi1Δ
WT
cuf1Δ
WT
#1
#2
ctr4Δ
lac1Δ
+ 10 µM BCS
+ 10 µM CuSO4
C
L-DOPA + 10 µM CuSO4
L-DOPA + 10 µM BCS
LAC1
Log2 fold change
WT=1
****
WT cuf1Δ WT #1 #2
ΔAce1
CUF1-FLAG
D
CTR4
Log2 fold change
WT=1
L-DOPA + 10 µM BCS
****
WT cuf1Δ WT #1 #2
ΔAce1
CUF1-FLAG

Figure 3

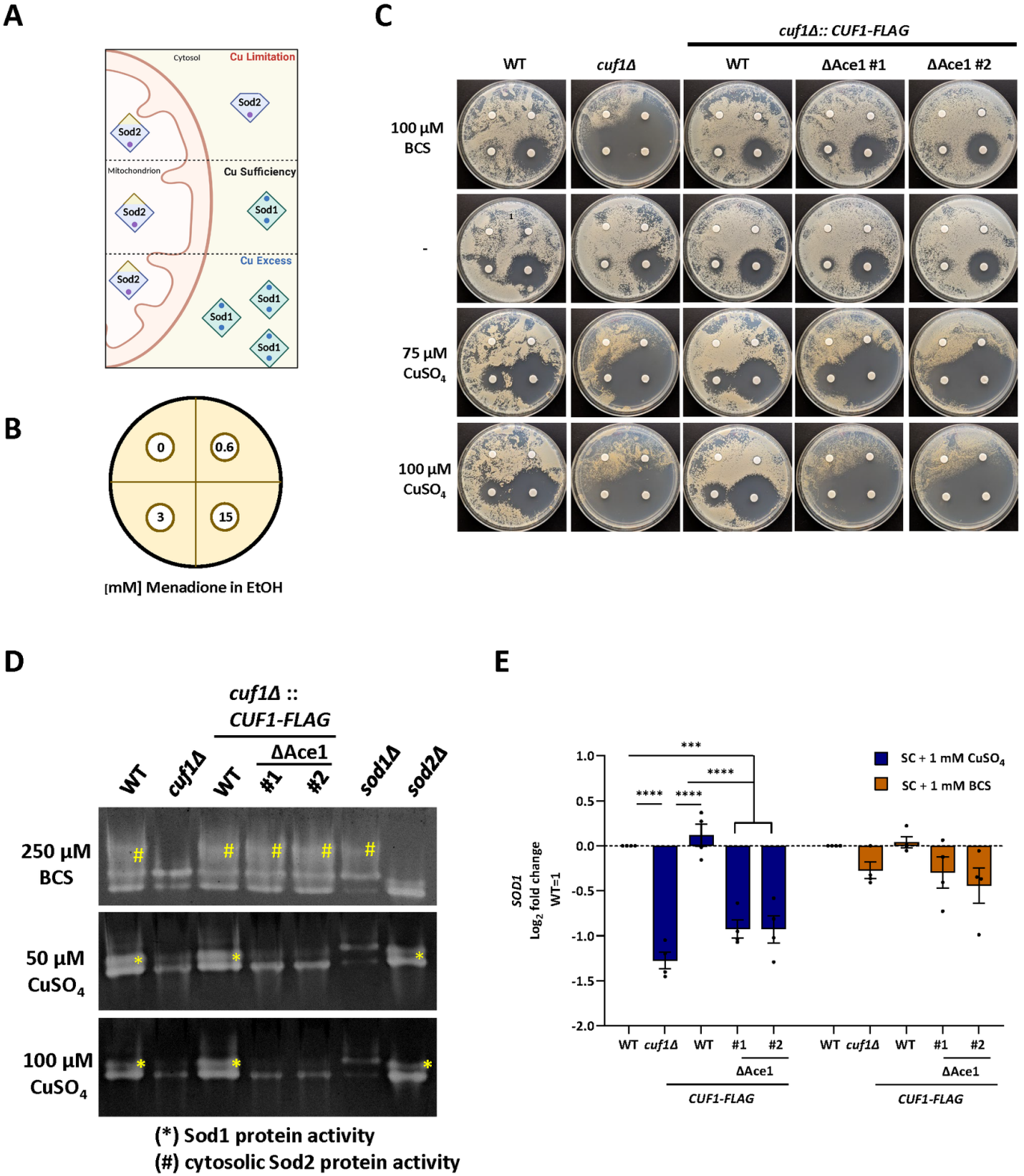
A
Cytosol
Cu Limitation
Sod2
Mitochondrion
Cu Sufficiency
Sod1
Cu Excess
B
0
0.6
3
15
[mM] Menadione in EtOH
C
cuf1Δ:: CUF1-FLAG
WT
cuf1Δ
WT
ΔAce1 #1
ΔAce1 #2
100 µM BCS
-
75 µM CuSO4
100 µM CuSO4
D
cuf1Δ :: CUF1-FLAG
ΔAce1
WT
cuf1Δ
WT
#1
#2
sod1Δ
sod2Δ
250 µM BCS
50 µM CuSO4
100 µM CuSO4
(*) Sod1 protein activity
(#) cytosolic Sod2 protein activity
E
SC + 1 mM CuSO4
SC + 1 mM BCS
SOD1 Log2 fold change WT=1
1.0
0.5
0.0
-0.5
-1.0
-1.5
-2.0
***
****
WT
cuf1Δ
WT
#1
#2
ΔAce1
CUF1-FLAG

Figure 4

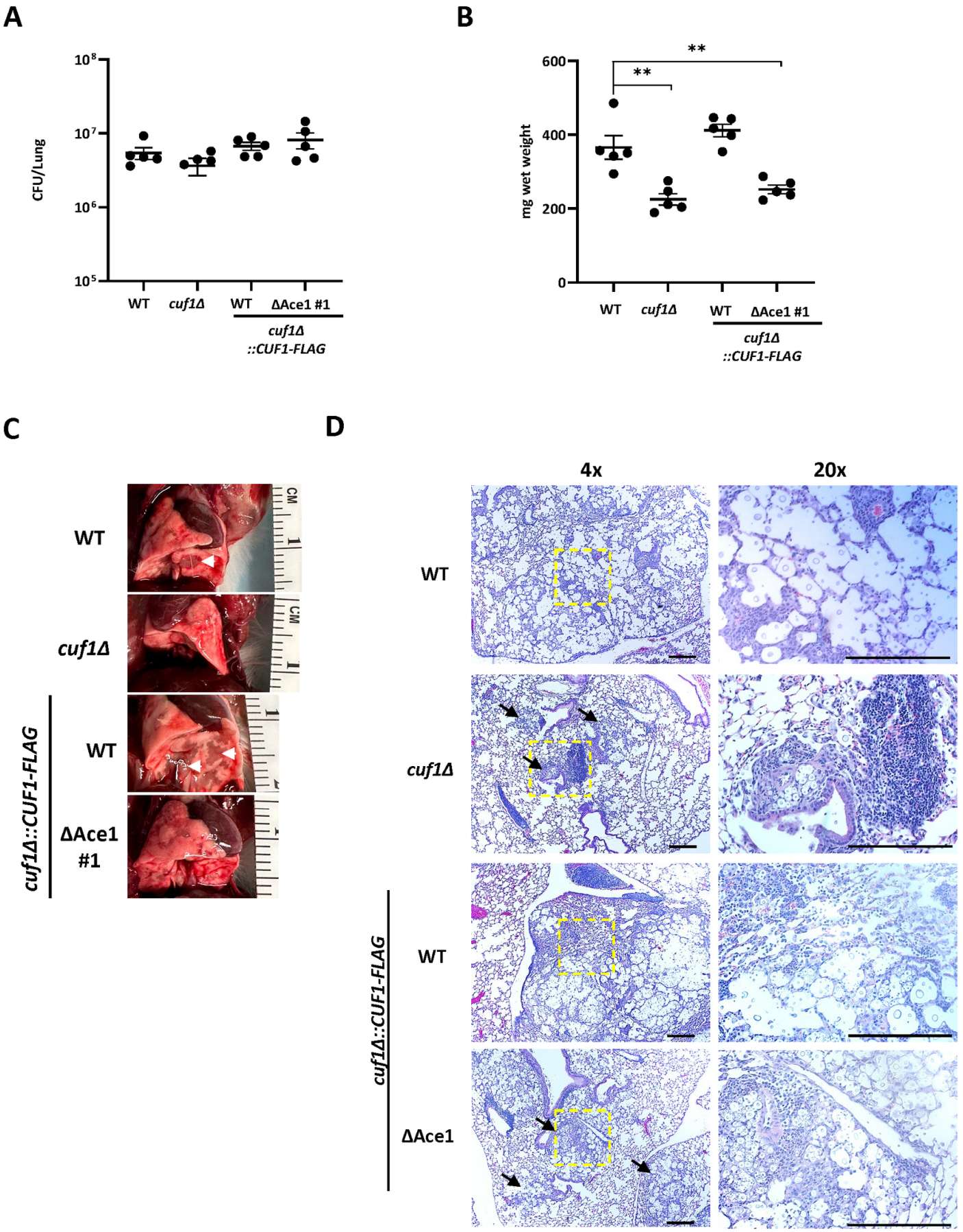
A
CFU/Lung
10^8
10^7
10^6
10^5
WT
cuf1Δ
WT
ΔAce1 #1
cuf1Δ
::CUF1-FLAG
B
mg wet weight
600
400
200
0
**
**
WT
cuf1Δ
WT
ΔAce1 #1
cuf1Δ
::CUF1-FLAG
C
WT
cuf1Δ
cuf1Δ::CUF1-FLAG
WT
ΔAce1
#1
D
4x
20x
WT
cuf1Δ
cuf1Δ::CUF1-FLAG
WT
ΔAce1

Figure 5